1977

The interactions of hydrogen with ethylene and ethane on iridium

Paul Robert Mahaffy
Iowa State University

INFORMATION TO USERS

This material was produced from a microfilm copy of the original document. While the most advanced technological means to photograph and reproduce this document have been used, the quality is heavily dependent upon the quality of the original submitted.

The following explanation of techniques is provided to help you understand markings or patterns which may appear on this reproduction.

1. The sign or "target" for pages apparently lacking from the document photographed is "Missing Page(s)". If it was possible to obtain the missing page(s) or section, they are spliced into the film along with adjacent pages. This may have necessitated cutting thru an image and duplicating adjacent pages to insure you complete continuity.

2. When an image on the film is obliterated with a large round black mark, it is an indication that the photographer suspected that the copy may have moved during exposure and thus cause a blurred image. You will find a good image of the page in the adjacent frame.

3. When a map, drawing or chart, etc., was part of the material being photographed the photographer followed a definite method in "sectioning" the material. It is customary to begin photoing at the upper left hand corner of a large sheet and to continue photoing from left to right in equal sections with a small overlap. If necessary, sectioning is continued again — beginning below the first row and continuing on until complete.

4. The majority of users indicate that the textual content is of greatest value, however, a somewhat higher quality reproduction could be made from "photographs" if essential to the understanding of the dissertation. Silver prints of "photographs" may be ordered at additional charge by writing the Order Department, giving the catalog number, title, author and specific pages you wish reproduced.

5. PLEASE NOTE: Some pages may have indistinct print. Filmed as received.

University Microfilms International
300 North Zeeb Road
Ann Arbor, Michigan 48106 USA
St. John's Road, Tyler's Green
High Wycombe, Bucks, England HP10 8HR

The interactions of hydrogen with ethylene and ethane on iridium

by

Paul Robert Mahaffy

A Dissertation Submitted to the
Graduate Faculty in Partial Fulfillment of
The Requirements for the Degree of
DOCTOR OF PHILOSOPHY

Department: Chemistry
Major: Physical Chemistry

Approved:

Signature was redacted for privacy.

In Charge of Major Work

Signature was redacted for privacy.

For the Major Department

Signature was redacted for privacy.

For the Graduate College

Iowa State University
Ames, Iowa

1977

TABLE OF CONTENTS

INTRODUCTION

The work described in the following pages attempts to establish the mechanisms of the catalytic addition of hydrogen to ethylene and ethane to produce, respectively, ethane and methane. The catalyst used was iridium, a transition metal of face centered cubic symmetry, prepared in such a way as to produce a surface clean on an atomic scale.

The complexity of the hydrocarbon-hydrogen-iridium system can be appreciated by slowly dosing pure ethylene onto a clean or hydrogen predosed iridium film (1, 2) (held at 100°C) of the type used in this study and observing the amounts of gas phase products with a quadrupole mass spectrometer as functions of time. Hydrogen, methane, ethane and eventually ethylene all appear in the gas phase but in concentrations which depend among other things on the ethylene dose rate.

Catalytic hydrogenation and hydrogenolysis of hydrocarbons are important reactions in many processes (for example, coal liquefaction, petroleum conversion processes, etc.) and it is not surprising that the addition reactions of hydrogen to these small hydrocarbons have been extensively studied. Nevertheless, controversy over mechanisms attests to the fact that these processes are not well understood. It is the viewpoint of the author that in the case of ethylene hydrogenation much of this confusion results from complications caused by the surface dehydrogenation of adsorbed ethylene--therefore, much of the work described herein pertaining to ethylene hydrogenation was carried out in a temperature region where the rate of surface dehydrogenation was negligible. In the case of ethane hydrogenolysis, it is simply felt that no experimental study has been

carried through in enough detail to adequately test a proposed mechanism. To carry out this investigation in such detail has had the disadvantage of limiting the study to one transition metal.

Iridium was chosen for several reasons. It is an active catalyst for both reactions; only a relatively small amount of kinetic work has been carried out on it, yet several adsorption studies have been completed which help characterize surface species on iridium important for these reactions.

The first part of this dissertation will survey literature relevant to each reaction. Following this, the experimental procedures used in this study will be described. Part 3 is a presentation and discussion of the results of this investigation.

LITERATURE REVIEW

Ethylene Hydrogenation

The catalytic hydrogenation of ethylene to produce ethane, discovered before the turn of the century by P. Sabatier and J. B. Senderens (3), has been one of the most extensively studied reactions in heterogeneous catalysis. The following paragraphs will survey a number of techniques used to characterize the reaction over transition metals, outline the main features of the results obtained from these techniques and summarize the hydrogenation mechanisms proposed to explain these results.

Heterogeneous catalytic systems are generally characterized, in part, by measurements of the overall rate of reaction as a function of temperature, partial pressures of reactants and products, and the type of catalyst used, including its preparation history. Since such kinetic measurements can, in general, only support but not prove a proposed sequence of elementary steps (a reaction mechanism), additional techniques are often used to disprove or support a mechanism consistent with the global kinetics. One such technique, that of isotope labeling, has assumed major importance in the study of ethylene hydrogenation, partly because of its easy applicability to the hydrogen ethylene system, but partly also because of the complicated often confusing kinetic results obtained by many workers in this field.

The use of isotope labeling of hydrogen atoms to study ethylene hydrogenation began in the early 1930's; the first experiments determined relative deuterium-hydrogen concentrations by following the thermal conductivity (4) or by measuring the density of water produced from the hydrogen

products of the reaction (5). In time mass spectral analytic techniques became readily available and the deuterium content of gas phase hydrogen, ethylene and ethane could be monitored. Isotope labeling of carbon made it possible to measure the extent of irreversible ethylene adsorption on various catalysts (6, 7).

Another set of technical developments which affected the direction of ethylene hydrogenation research was the development and application of thin film technology to catalysis. This work was pioneered by O. Beeck in the mid-1940's (8) and along with the development of ultra high vacuum techniques was considered to be a major development in the science of catalysis. With suitable experimental care, thin films of transition metals could now be prepared in ultra high vacuum, resulting in an atomically clean catalytic surface before introduction of reactants.

Results of experiments of the above type have been described in reviews (9, 10). A few characteristic features of the hydrogenation reaction are discussed below. The greatest part of this work was carried out over nickel catalysts.

As indicated above, an easy interpretation of much of the kinetic work carried out on the ethylene hydrogenation reaction has been hindered by changes in the catalytic activity with time. In addition to the usual problems of irreproducibility caused by poisoning of the catalytic surface by impurities, sintering, etc., it appears that under certain conditions the hydrogenation reaction is poisoned by surface dehydrogenation of ethylene. This was illustrated in early work (11) by a dependence of the rate on the order in which the reactants were introduced to the surface. The

hydrogenation was more rapid if hydrogen was introduced to the catalyst prior to the ethylene dose.

Furthermore, if small sequential doses of ethylene, but no hydrogen, are added to a thin film generated under vacuum conditions, it is often observed (12, 13, 14, 15, 2) that the initial gas phase products (which only appear after several such doses) are some combination of ethane, hydrogen and methane. For a given catalyst, film temperature and dose size, one, two or all three of these products may appear. Of course, if the dosing is continued ethylene will also eventually appear in the gas phase.

K. Miyahara points out differences in the activities of clean and "carbided" (or ethylene pretreated) surfaces for hydrogenation and exchange (16) and J. G. Foss and H. Eyring (17) have shown that treatment of a carbided Ni surface with hydrogen partially restores the activity. It appears that in some cases a certain amount of adsorbed carbon remains irreversibly bound to the surface (6, 7).

Another feature of the hydrogenation kinetics often observed is that the rate as a function of temperature passes through a maximum (or relative maximum) at some point Tm. Early speculation as to the mechanistic cause for this behavior included olefin desorption (18) or a shift in the rate limiting step from hydrogen adsorption to $C_2H_5(a)$ hydrogenation (19). Another suggestion was that Tm was caused by the destruction of a reactive intermediate by its further dehydrogenation. In certain cases the experimental evidence has supported this viewpoint. For example, on W films Miyahara et al. observed Tm to be $\sim$ 300 K (20). Moreover at 228 K on addition of D_2 and C_2H_4, these authors observed relatively slow

hydrogenation and rapid ethylene exchange. This seemed surprising since earlier in carrying out essentially the same experiment at 173 K over W, C. Kemball (21) had observed an exchange rate near zero but a relatively good hydrogenation activity to produce predominantly $C_2H_4D_2$. R. Rye then suggested (22) that in light of thermal desorption and self-hydrogenation experiments (23, 24) (carried out by adsorbing ethylene on polycrystalline W wires), the results could be explained by postulating a two-step surface dehydrogenation of ethylene

$$C_2H_4(a) \rightleftharpoons C_2H_2(a) + 2\,H(a)$$

$$C_2H_2(a) \rightleftharpoons C_2(a) + 2\,H(a) \quad .$$

The rate of the first reaction would become important at $\sim$ 200 K and would account for the differences in the isotope labeling experiments of Kemball and Miyahara described above, while the rate of the second reaction would become significant at T $\sim$ 300 K and account for Tm $\sim$ 300 K as observed by Miyahara. If this were indeed the case, one might also expect to see a deviation from the normal temperature dependence of the rate at $\sim$ 200 K. This temperature range was, however, not covered in the experiments of Miyahara.

A number of ethylene hydrogenation mechanisms have been proposed. Those of the Rideal-Eley type include elementary steps such as reaction of gas phase ethylene with hydrogen atoms adsorbed on adjacent surface sites (25), reaction of gas phase hydrogen with adsorbed ethylene (26, 27) and direct abstraction of two hydrogen atoms from an adsorbed surface ethylene by an impinging gas phase ethylene molecule (28). Mechanisms of the Langmuir-Hinshelwood type include hydrogen transfer between an adsorbed

ethylene molecule and a dehydrogenated $C_2H_4(a)$ species (29), reaction between adsorbed ethylene and adsorbed hydrogen molecules (30) and a two-step addition of hydrogen atoms to adsorbed ethylene, formulated by Horiuti and Polanyi (31) as

$$\begin{array}{l} C_2H_4 \xrightarrow{I_a} C_2H_4(a) \\ H_2 \xrightarrow{I_b} H(a) + H(a) \end{array} \Bigg\} \xrightarrow{II} C_2H_5(a) \Bigg\} \xrightarrow{III} C_2H_6$$

This last mechanism has the advantage that by allowing certain steps to be slow or reversible, one can in many cases account for the distribution of deuterium in the reactants and products when D_2 and C_2H_4 interact with the catalyst. In a number of cases the other mechanisms listed cannot account for the results of the isotope labeling experiments. A weakness of the Horiuti-Polanyi mechanism is that it ignores effects of surface dehydrogenation on rates and isotope distributions.

Various surface probes (I.R., U.P.S., L.E.E.D., etc.) have dealt with the problem of the electronic and geometric structure of surface species resulting from ethylene adsorption on transition metal surfaces. It should, of course, be kept in mind that, in general, these experiments are not carried out under reaction conditions, therefore, the results obtained may not reflect the condition of the surface during the steady state catalytic reaction. Support for the existence of an intermediate in the Horiuti-Polanyi hydrogenation mechanism, the ethyl radical $C_2H_5(a)$, has come particularly from infrared studies (32, 33, 34) where methyl stretching modes observed on addition of ethylene or ethylene and hydrogen to silica supported Ni, Co and Pd have been interpreted as $C_2H_5(a)$ or

$(CH_2)n\ CH_3(a)$ (with $n \sim 3$). In general, the extent of saturation observed upon dosing ethylene is enhanced by hydrogen addition.

These results are to be compared to the report of J. Demuth and D. Eastman (35) of U.P.S. spectra of ethylene adsorbed on Ni (111) in which they report shifts in the energy of π electron levels relative to condensed and gaseous ethylene, which are interpreted in terms of π-d bonding to the surface. As the temperature of the crystal is raised through 230 K, the adsorbed ethylene spectrum changes to a spectrum identical to the adsorbed acetylene spectrum. At 470 K the authors find evidence for the formation of a "carbonaceous species." Model calculations (36) suggest that the U.P.S. results of Eastman cannot in themselves distinguish between a π complex coordinated to a single atom and a di - σ - adsorbed ethylene, because in both cases the energy of the highest occupied π orbital is shifted due to interaction with the Ni surface. Other attempts to model ethylene adsorption include CFSO-BEBO calculations by W. Weinberg et al. on the Pt (111) surface (37).

Baron et al. have used low energy electron diffraction in combination with Auger electron spectroscopy to study ethylene adsorption particularly on a series of stepped and low index Pt surfaces (38) but also on Ir (111) and Ir[6(111) x (100)] (39). The extent of dehydrogenation or decomposition and formation of ordered surface species at a given temperature is found to be a strong function of the surface geometry and the number and type of steps. However, overshadowing these effects are differences between Pt and Ir (caused by electronic effects since the crystal parameters of Ir and Pt are very similar). For example, surface dehydrogenation of ethylene occurred on Ir at room temperature even on the close packed

(111) surface, and only trace amounts of carbon were removed from the surface upon thermal desorption, in contrast to Pt (111) where a considerable fraction of the ethylene adsorbed could be desorbed as ethylene. Somorjai does not attempt to provide any detailed explanations for either the L.E.E.D. patterns observed or their temperature dependence.

Of particular relevance to the ethylene hydrogenation work described in this dissertation are experimental results obtained by J. R. Arthur and R. S. Hansen (40) using field emission techniques to study the adsorption of ethylene, acetylene and hydrogen on Ir. Changes in the work function ($\Delta\phi$) of the tip upon adsorption at 4 K are measured for each of these gases from the experimentally observed I-V curves. Subsequent to this determination in each case the tip was heated for 20 s to a higher temperature with the field off, then recooled to again measure the work function shift. Some of these results are shown in Figures 1-4. Hydrogen causes an increase in the work function, its desorption which begins just below 200 K causes the work function to return to the clean value. Adsorption of either acetylene or ethylene (this occurs irreversibly) causes a decrease in the work function. The $\Delta\phi$ (T) plots for the latter show a sharp increase at T $\sim$ 150 K that is attributed to surface dehydrogenation of ethylene to form adsorbed acetylene and adsorbed hydrogen. The adsorbed acetylene does not begin to lose hydrogen at an appreciable rate until T $\sim$ 400 k; the ethylene and acetylene curves become similar in shape at this point. These results are all consistent with thermal desorption results carried out on a pollycrystalline Ir wire (41) and provide a good indication of the temperatures at which the rates of various surface dehydrogenation processes become important. Work function changes have been

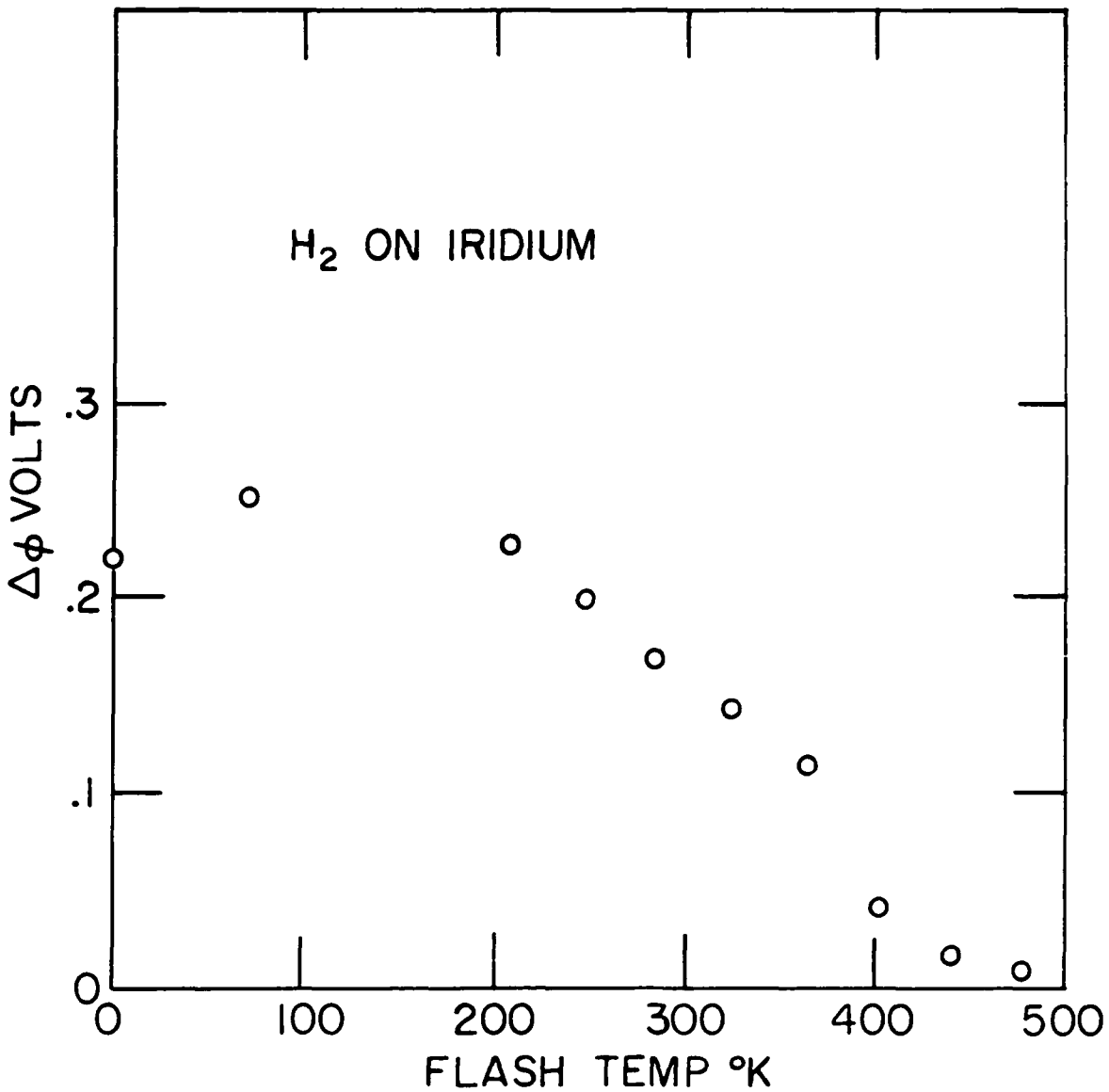

Figure 1. Results of Arthur and Hansen (40) showing the change in work function with temperature for hydrogen adsorbed on iridium

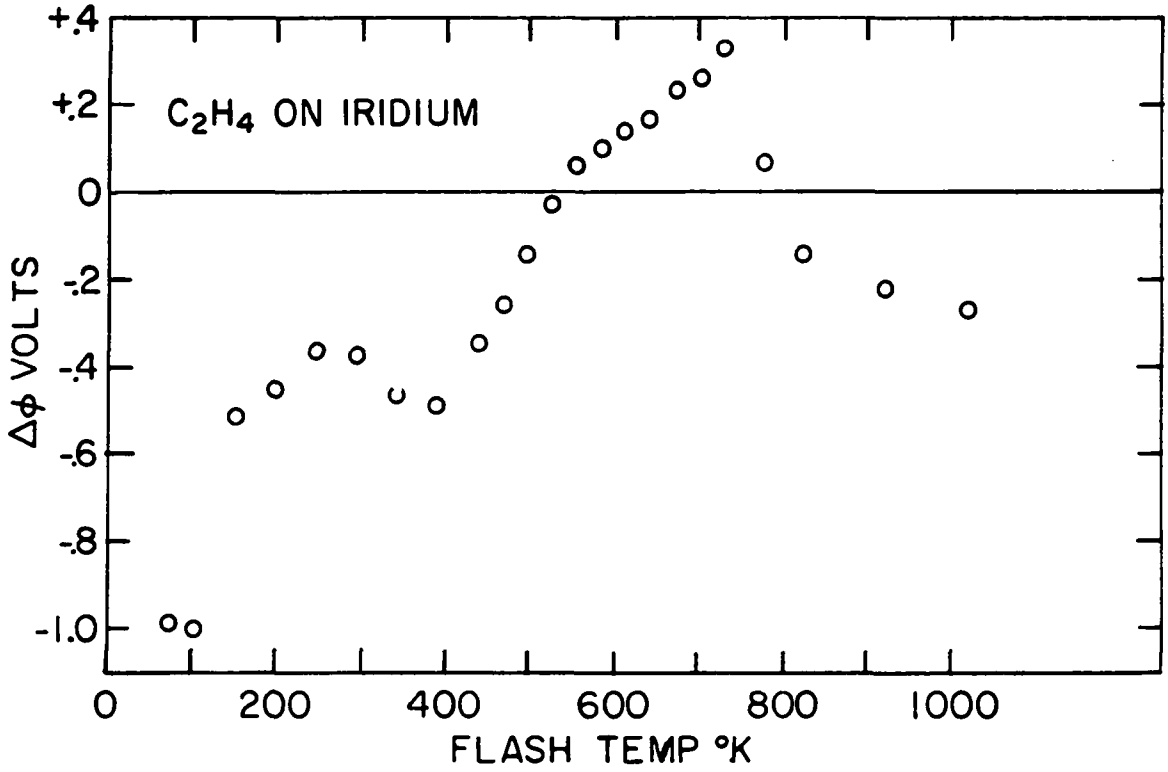

Figure 2. Results of Arthur and Hansen (40) showing the change in work function (obtained from the Fowler-Nordheim plot) with temperature for ethylene adsorbed on iridium

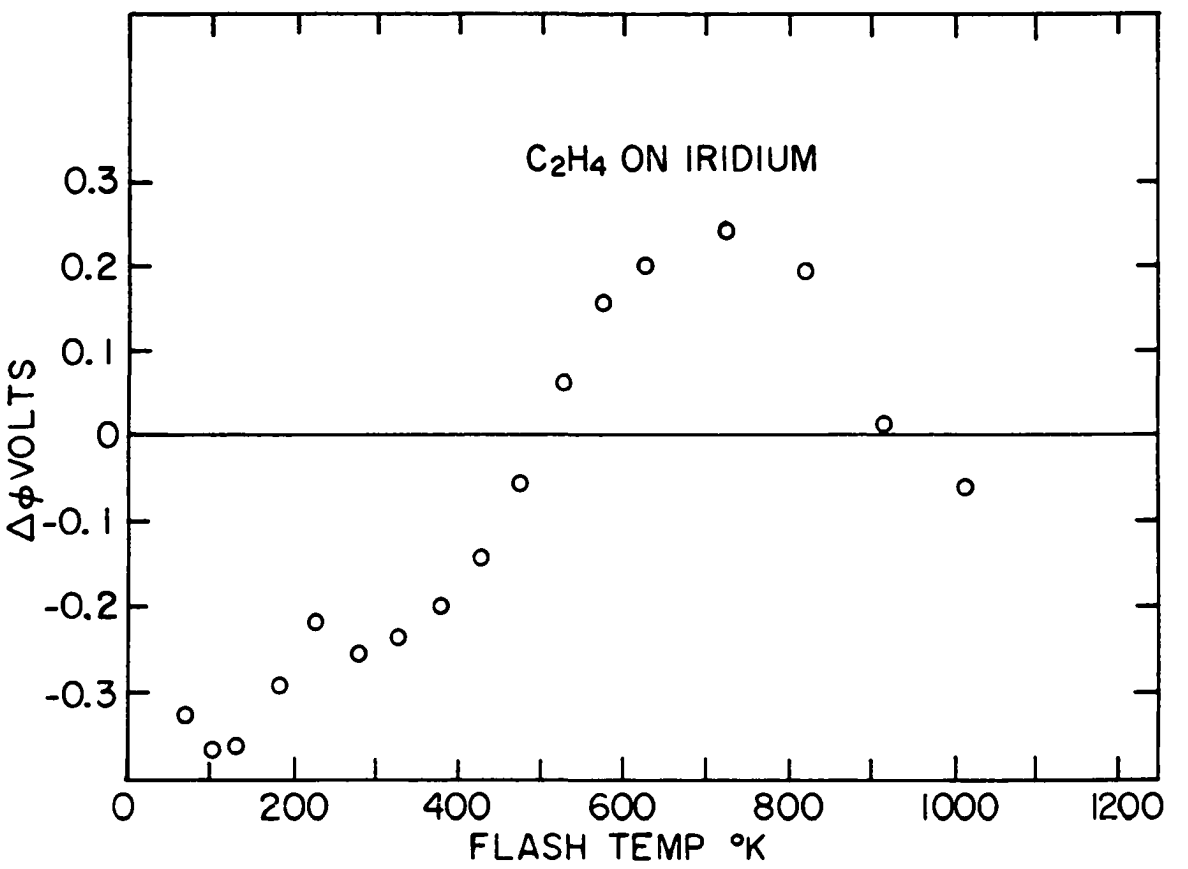

Figure 3. Results of Arthur and Hansen (40) showing the change in work function with temperature for ethylene adsorbed on iridium. In this case the work function change is estimated by another method

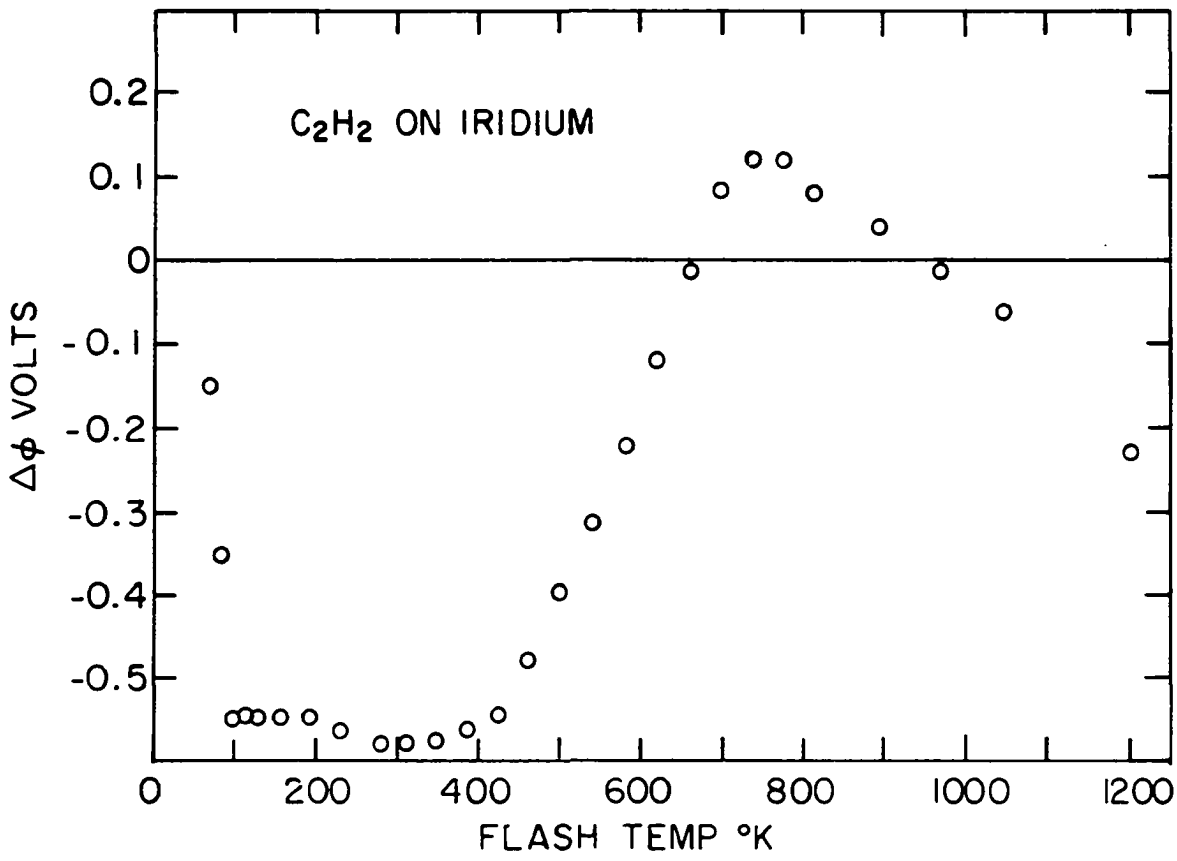

Figure 4. Results of Arthur and Hansen (40) showing the change in work function with temperature for acetylene adsorbed on iridium. $\Delta\phi$ is obtained by the same method as in Figure 3

measured upon ethylene adsorption on Ni, Pd, Pt, Cu, Au and Al thin films (42), the interpretation is not, however, in this case straightforward as all these experiments were carried out at only one temperature, 293 K.

Ethane Hydrogenolysis

The hydrogenolysis of ethane to produce methane has been studied much less extensively than the ethylene hydrogenation reaction. However, both thin films and supported catalysts have been used in work done and a number of hydrogenolysis mechanisms have been proposed. Over the conditions of temperature and partial pressures of reactants used in these studies and in the cases where kinetic information was obtained, the rate of reaction was, in general, found to be negative order in hydrogen pressure and positive order in ethane pressure with a fairly high apparent activation energy $\sim$ 25 to 40 kcal/mole. Modern surface techniques such as L.E.E.D., X.P.S., U.P.S., etc. have not been applied to ethane adsorption, primarily because its low sticking probability makes its adsorption very slow at the pressures normally used in these studies.

The first work on ethane hydrogenolysis was done by Kemball and Taylor (43) and Cimino et al. (44) who studied the reaction over Fe, Co and Ni supported catalysts. If the rate limiting step of the reaction was assumed to be the breaking of a carbon-carbon bond of a surface species C_2H_x (where $0 \leq x \leq 5$) in equilibrium with gas phase ethane, Taylor could explain the negative reaction order in hydrogen pressure and the positive order in ethane pressure. This reaction mechanism with slight (kinetically insignificant) modifications was used later by J. H. Sinfelt (45, 46) to explain his results on group VIII metals (47, 48, 49, 50, 51). Because this is one

of the few detailed mechanistic proposals (it takes into account observations of a variable hydrogen to carbon ratio on the surface of different metals) and because Sinfelt proposes to explain his observed kinetics of hydrogenolysis over most of the group VIII metals in terms of this mechanism, it is worthwhile to examine this formulation in some detail.

The proposed reaction steps are as follows:

1. $C_2H_6(g) \underset{k_{-1}}{\overset{k_1}{\rightleftharpoons}} C_2H_5(a) + H(a)$

2. $C_2H_5(a) + H(a) \underset{k_{-2}}{\overset{k_2}{\rightleftharpoons}} C_2H_x(a) + a\ H_2(g)$ with $a = \frac{6 - x}{2}$

3. $C_2H_x(a) \xrightarrow{k} C\ H_y(a) + C\ H_z(a)$

4. $C\ H_y(a) + C\ H_z(a) \xrightarrow[\text{fast}]{H_2} 2\ C\ H_4(g)$ (a)

Step 3 is taken to be the rate limiting process. If step 2 is in equilibrium then

$$K_{eq} = \frac{[C_2H_x(a)]\ [H_2(g)]^a}{[C_2H_5(a)]\ [H(a)]}$$

$$[C_2H_x(a)] = \frac{K_{eq}\ [H(a)]\ [C_2H_5(a)]}{[H_2(g)]^a} \qquad \text{(b)}$$

If there is a constant amount of carbon on the surface,

$$k_1\ [C_2H_6(g)] - k_{-1}\ [C_2H_5(a)]\ [H(a)] - k\ [C_2H_x(a)] = 0$$

or on substituting eq. (b) in the above,

$$[C_2H_5(a)]\ [H(a)] = \frac{k_1\ [C_2H_6(g)]}{k_{-1} + k\ K_{eq}/[H_2(g)]^a} \qquad \text{(c)}$$

$$r \equiv -\frac{d\,[C_2H_6(g)]}{dt} = k\,[C_2H_x(a)]$$

$$= \frac{k_1\,[C_2H_6(g)]}{\left[\frac{k_{-1}}{k\,K_{eq}}\,[H_2(g)]^a + 1\right]} \qquad (d)$$

by (b) and (c).

Among the assumptions of the preceding derivation are the following:

(i) Step 3 is rate determining.

(ii) Gas phase ethane is in equilibrium with the dehydrogenated surface species $C_2H_x(a)$.

(iii) The surface coverage of all species is low so that ethane is not in competition with hydrogen for sites.

That assumption (iii) is necessary to obtain (d) can be easily seen if step 1 is more correctly written as

$$C_2H_6(g) + 2\,* \underset{k_{-1}}{\overset{k_1}{\rightleftharpoons}} C_2H_5(a) + H(a)$$

where * designates an unoccupied adsorption site. Then, since steps 2 and 3 do not involve [*], the rate becomes

$$r = \frac{K_1\,[C_2H_6(g)]\,[*]^2}{\left[\frac{k_{-1}}{k\,K_{eq}}\,[H_2(g)]^a + 1\right]} \qquad (d)'$$

which will be first order in ethane pressure only when (iii) holds and [*] is constant.

Over a silica supported cobalt catalyst, Sinfelt and Taylor (51) have observed the rate to be fairly well described by (d) over a 60° temperature range and a fairly small range of partial pressures of hydrogen and ethane.

If the $C_2H_x(a)$ species were $C_2H_4(a)$, a should equal 1.0. The experimentally observed value of a was 0.8 while the order in ethane pressure was 1.0. Sinfelt also considers the consequences of the rate determining step involving an impinging gaseous hydrogen molecule. Then step 3 is modified to

$$3.' \qquad C_2H_x(a) + H_2(g) \longrightarrow C\,H_y(a) + C\,H_z(a)$$

and the derivation of

$$r = k\,[C_2H_x(a)]\,[H_2(g)]$$

$$= \frac{k_1\,[C_2H_6(g)]}{\left[\frac{k_{-1}}{k\,K_{eq}}\,[H_2(g)]^{a-1} + 1\right]}$$

or

$$r' = \frac{k_1\,[C_2H_6(g)]\,[*]^2}{\left[\frac{k_{-1}}{k\,K_{eq}}\,[H_2(g)]^{a-1} + 1\right]}$$

follows immediately. In this case, of course, the observed exponent on $[H_2(g)]$, $a - 1 = .8 \cong 1$ means that the carbon species involved in the carbon-carbon bond rupture is $C_2H_2(a)$, not $C_2H_4(a)$. Sinfelt feels that the rate determining step involving no gas phase hydrogen best describes the kinetics on the greatest number of metals studied.

Either of the two possible mechanisms described above should give a first order dependence of the rate on ethane pressure. Of the eleven silica supported metals studied by Sinfelt, however, more than half had an ethane pressure exponent of between 0.5 and 0.8. A possible explanation is that in these cases assumption (iii) is not valid and an appreciable fraction of the surface is covered. To proceed further one must then use an

adsorption model to evaluate [*] in (d)'. Sinfelt does this by replacing $[C_2H_x(a)]$ in the rate expression by

$$\frac{K\,[C_2H_6(g)] \,/\, [H_2(g)]^a}{1 + K\,[C_2H_6] \,/\, [H_2(g)]^a}$$

and by using the approximation

$$\theta_x = \frac{b\,P_x}{1 + b\,P_x} \cong (b\,P_x)^n \quad 0 \leq n \leq 1$$

to evaluate his data. When this is done

$$r = \left[K \frac{[C_2H_6(g)]}{[H_2(g)]^a} \right]^n \tag{e}$$

and the value of a (assumed to be equal to 1, 2 or 3) can be chosen to give the best fit to -an. On the silica supported metals studied by Sinfelt, the hydrogen pressure exponent calculated by the above procedure ranges from -1.0 to -2.7 and differs by 0.25 on the average from the experimentally observed value of this exponent.

This discrepancy could in part be due to Sinfelt's approximation

$$r = \frac{K\,[C_2H_6(g)] \,/\, [H_2(g)]^a}{1 + K\,[C_2H_6(g)] \,/\, [H_2(g)]^a} \cong \left[K \frac{[C_2H_6(g)]}{[H_2(g)]^a} \right]^n$$

but the small range of partial pressures covered in Sinfelt's experiments does not allow for an adequate test of either of these expressions.

C. Kemball (52) has criticized Sinfelt's formulation by pointing out that

$$[C_2H_x(a)] = \frac{K\,[C_2H_6(g)] \big/ [H_2(g)]^a}{1 + K\,[C_2H_6(g)] \big/ [H_2(g)]^a}$$

is not necessarily the correct Langmuir expression if there are other hydrocarbon and hydrogen species competing for the same sites. For example, if the surface species were $C_2H_5(a)$, $C_2H_4(a)$ and $H(a)$, all in equilibrium, then

$$\theta_{C_2H_4(a)} = \frac{a\,[C_2H_4(g)]}{1 + a\,[C_2H_4(g)] + b\,[C_2H_5(g)] + c\,[H(g)]}$$

$$= \frac{a'\,[C_2H_6] \big/ [H_2]}{1 + a'\,[C_2H_6] \big/ [H_2] + b'\,[C_2H_6] \big/ [H_2]^{1/2} + c'\,[H_2]^{1/2}}$$

where a', b' and c' now include the equilibrium constants for the gas phase equilibration of each of these species. According to Sinfelt's mechanism $r \sim \theta_{C_2H_4(a)}$ when $a = 1$ so this expression could be experimentally tested.

M. Boudart (53) has questioned the probability of extensively dehydrogenated $C_2H_x(a)$ species being in equilibrium with gas phase ethane as suggested by the Sinfelt-Taylor mechanism. Instead he proposes irreversible dissociative adsorption of ethane onto a nonuniform surface and an irreversible step in which the carbon-carbon bond is broken by a reaction of $H_2(g)$ with $C_2H_x(a)$. Considering hydrogen adsorption to be on sites where carbon does not adsorb and by using the rate law for a two-step reaction on a nonuniform surface as developed by S. Khammouma (54), Boudart derives a rate law which turns out to be of the same form as eq (e). Thus, to distinguish between the Boudart and Sinfelt-Taylor mechanisms, techniques such

as isotope labeling are needed in addition to the measurements of the reaction orders.

In contrast to the mechanisms described above, Anderson and Baker (55) studied the hydrogenolysis of ethane over films of Ni, Fe and W and concluded, from similarities in the temperature dependence of the rates of hydrogenolysis and methane exchange, that the hydrogenolysis was desorption controlled. They cited as further evidence the low rate of ethane exchange as compared to methane formation during the hydrogenolysis. On the other hand, no attempt was made to explain the dependence of the rate on a negative exponent of the hydrogen pressure as observed by Taylor and Sinfelt, and in fact in this study these authors did not even measure the reaction order in hydrogen pressure. In addition, recent work by L. Guczi et al. (56) again over Ni produced results which seem to contradict the conclusions of Anderson. These authors studied the temperature dependence of ethane exchange and hydrogenolysis using D_2 in the place of hydrogen over a large temperature range ($170^{\circ}C$-$320^{\circ}C$). As the temperature was raised, the mean deuterium number of the initial methane product decreased while the mean deuterium number of the ethane increased as a result of faster ethane exchange. If desorption was the rate limiting step, these mean deuterium number changes should be in the same direction. Furthermore, Guczi found the activation energy for methane desorption from the surface to be significantly lower than E_a for the hydrogenolysis reaction, again suggesting desorption is not the rate limiting step.

In summary, in the ethane hydrogenolysis work described, the kinetic measurements carried out do not provide an adequate test of the mechanisms proposed. This is due partially to the narrow reactant pressure ranges

covered in these studies and partially due to the inadequate development of a rate law from the proposed mechanisms. Supplemental techniques are also needed to get a better handle on the reaction mechanism.

EXPERIMENTAL

The system designed to carry out the kinetic experiments consisted of mercury diffusion pumps and ion pumps capable of producing ultra high vacuum conditions, partial and total pressure measuring devices and a stainless steel, pyrex reaction chamber which could be isolated from the pumps. The catalyst consisted of either a thin film of Ir prepared under ultra high vacuum conditions or Ir single crystals. The experimental apparatus and procedures are described in detail below.

Figure 5 is a schematic of the system. The principal pressure measuring devices are the Bayard-Alpert ionization gauges, a capacitance manometer covering the pressure range $\sim$ .1 to 1000 μ and a quadrupole mass spectrometer capable of measuring partial pressures in the 10^{-10} to 10^{-5} torr range. M-1, M-2 and M-3 are single, double and triple stage mercury diffusion pumps, while IP is an ion pump. The entire system could be baked to 400°C to remove background water vapor.

Generally, the first step in making a rate measurement was to meter an appropriate amount of reactant gas from a storage flask into the manifold volume (defined in Figure 5 by the more darkly shaded area) where the overall pressure was measured by the capacitance manometer. When C-2 was opened, a small amount of gas was continuously leaked from the manifold volume through a capillary and past the mass spectrometer where partial pressures could be measured. The linearity of capacitance manometer pressure with mass spectrometer ion current was checked for each gas over the range of pressures studied. The dose was then administered to the catalyst by opening valve C-1 whereupon the manometer served to monitor total

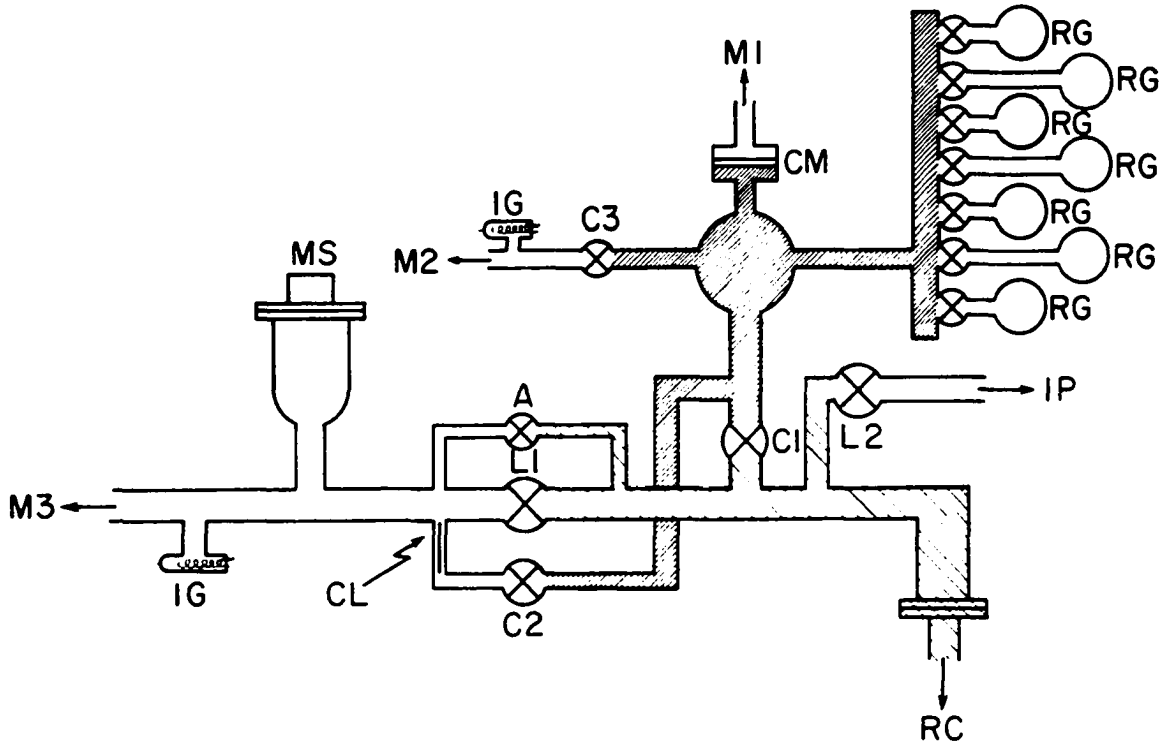

Figure 5. Schematic of the high vacuum system showing the quadrupole mass spectrometer (MS), capillary leak (CL), leak valve (A), standard U.H.V. valves (C1, C2, C3 and C), high conduction valves (L1, L2), ion gauges (IG), mercury diffusion pumps (M1, M2, M3), ion pump (IP), gas storage flasks (RG), capacitance manometer (CM) and reaction chamber (RC)

pressure during reaction and the mass spectrometer, partial pressures. The size of the capillary leak was such that over a typical reaction time period a negligible fraction of reactants would be lost through the leak. Thus the total shaded area was the reaction volume for an essentially static reactor.

The thin film catalyst surfaces were prepared by resistively heating a 5 or 10 mil iridium filament in ultra high vacuum in order to evaporate the metal on the walls of the pyrex cell (Figure 6). The cell was generally thermostatted to 100°C with boiling water during film deposition. The temperature of the filament was raised in small steps so that the wire would outgas thoroughly before the evaporation rate became significant. A 5-sec-on/5-sec-off heating cycle was used to minimize outgassing of the Ni supports to which the iridium wire was welded.

The iridium single crystal surfaces were cleaned by sequences of heating to 700°C in 5×10^{-7} torr oxygen, Ar^+ bombardment and electron bombardment heating in vacuum to 1200°C. The procedures used to clean the surfaces have been shown (39) to produce atomically clean iridium surfaces as determined by L.E.E.D. and Auger electron spectroscopy.

A diagram of each reaction chamber is shown in Figure 6. In the single crystal cell, two discs could be mounted at one time. Ar^+ bombardment was made possible by positioning a thoria coated iridium filament close to both of the crystals. 2×10^{-4} torr of pure argon was introduced to the cell, at which point +300 and -300 volts were applied to each crystal and the filament was resistively heated until the ion current at the negatively charged crystal was $\sim$ 10 μA. A five-minute bombardment time was considered sufficient to strip several layers of atoms from the surface.

Figure 6. Schematic of the thin film and single crystal reaction chamber

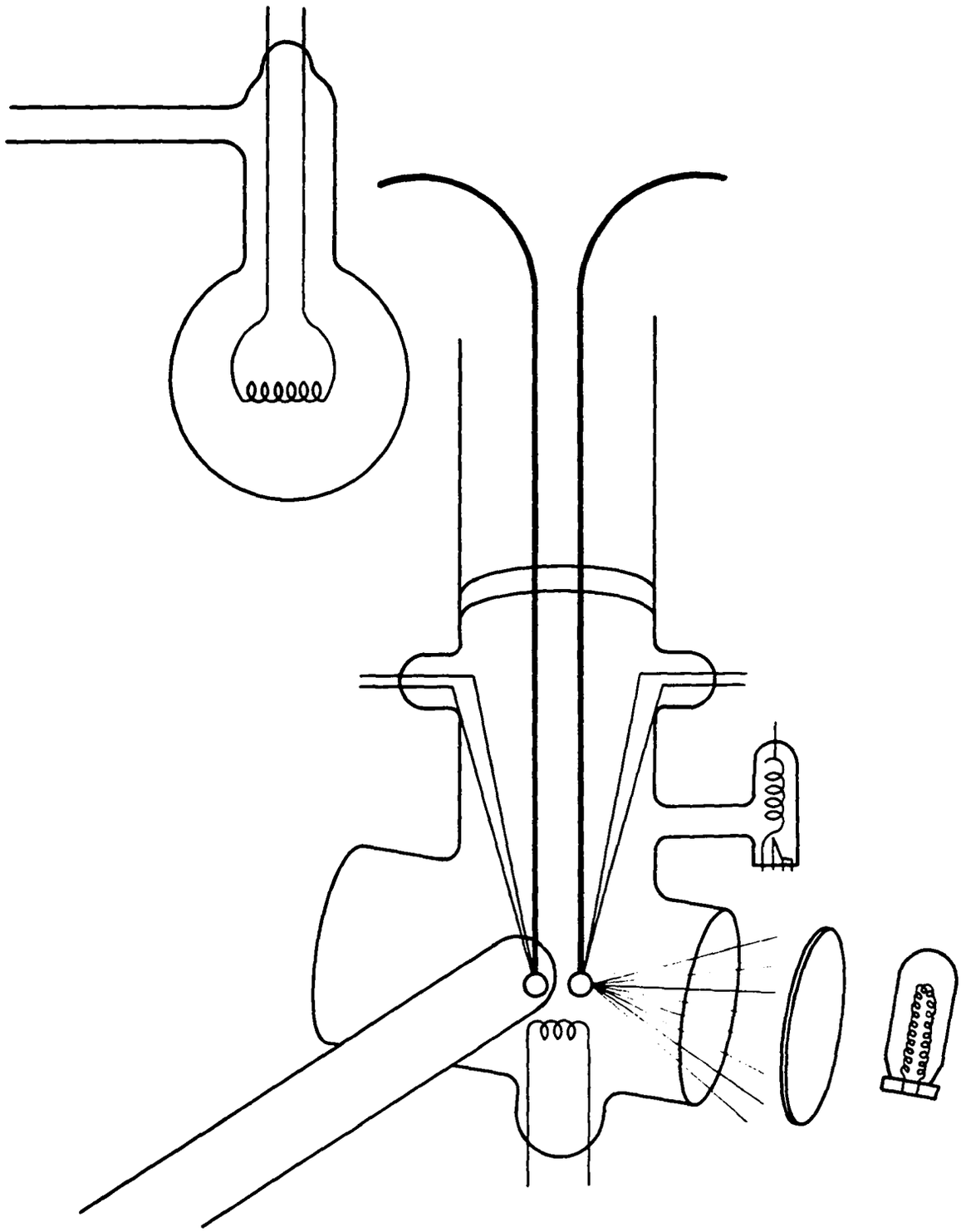

Electron bombardment heating was carried out by applying $\sim$ + 400 volts D.C. with respect to the filament to one or both of the crystals and heating the filament until the required electron emission was obtained. The temperature of each crystal was measured by means of a 3 mil W/5%, 26% Re set of thermocouple wires spotwelded to the edge of each crystal and by using an optical pyrometer for temperatures greater than 900°C.

During a catalytic run, the crystal was heated by focusing light from a filament in a bulb with a lens onto one of the crystal faces. As shown in Figure 6, the cell was built with a glass plate on each end to allow for the possibility of heating a crystal with two bulbs. The maximum temperature obtained under these conditions was $\sim$ 750°C in vacuum.

The iridium film, on the other hand, was thermostatted by immersion of the pyrex flask in a liquid bath maintained at the appropriate temperature. Between 0°C and 100°C a water bath was used; above 100°C the temperature of the film was controlled by either an oil bath or a molten salt bath (18 mole % $NaNO_3$, 30 mole % $LiNO_3$ and 52 mole % KNO_3). For temperatures in the range -73°C to -163°C, liquid-solid slurries of organic compounds (e.g. n-pentane, n-hexane or combinations of their isomers) could be prepared by adding small sequential amounts of liquid nitrogen to these organic liquids. The temperature could be controlled to within $\sim \pm$ 1 degree, at temperatures greater than the freezing point of the organic liquid, by stirring with a magnetic stirrer and adjusting the leak rate of liquid nitrogen into the bath. In general, after each experiment or series of experiments had been completed, the thin film bulb would be cut off and replaced and the system baked before another run could be carried out.

Some characteristics of iridium thin films prepared in vacuum at 100°C were investigated by P. B. Masterson (2). Using his terminology "film thickness" refers to the thickness a given weight of film would have if it was spread uniformly over the 300 cm^2 macroscopic surface area of the 500 ml flask and if the specific gravity of the film was 22.4 (the actual films are probably less dense, however). Over a thickness range 30-300° A, the surface area of the film as measured by hydrogen adsorption (and catalytic activity) was found by Masterson to be directly proportional to film thickness. Since this proportionality was well established (for a film deposition temperature of 100°C), it was not necessary to directly measure the amount of Ir deposited after each experiment.

The manifold and reaction cell volumes (Vm and Vc, respectively) were measured by expanding Ar from Vm into an empty gas storage bulb with a known volume. From the capacitance manometer pressure changes upon expansion, Vm could be calculated. Another expansion of Ar from Vm into Vc allowed a determination of Vc. These volumes changed slightly whenever the system was modified but remained close to 0.4 l (Vm) and 1.0 l (Vc).

The steps involved in measuring the amount of hydrogen adsorption following the deposition of a fresh film were very similar to those above. From the known volumes and temperatures and observed pressure changes upon expansion from Vm, the amount of hydrogen adsorbed on the surface could readily be determined.

The mass spectrometer (Electronic Associates, Inc., model Quad 150) operated in the pressure range 10^{-10} to 10^{-5} torr. The energy of the ionizing electrons was 75 volts and ions were screened from the electron multiplier by a high frequency electrical quadrupole field mass filter.

The mass range of the instrument was 1 to 150 a.m.u. and could be swept in milliseconds if the oscilloscope (Tectronix, Inc., type R.M. 503) was used to record the electron multiplier signal or in seconds if the two-channel, time-drive chart recorder (Brush Instruments, model Mark 780) was used. Most of the background impurities as well as the reactants and products encountered in this study were in the mass range 1-44 a.m.u.

The response time of the mass spectrometer for pressure changes made on the reaction chamber side of the capillary leak was on the order of a second or less for all gases except ethylene. Ethylene interacted enough with the pyrex walls to prevent its reaching equilibrium for several minutes. Thus it was not possible to measure rapid changes in ethylene's partial pressure in a mixture of several gases except by difference.

The relationship between the observed mass spectrometer ion current for a given atomic mass unit and the pressure in the reaction cell for a given species could in general be determined by direct calibration against the capacitance manometer. However, in the case of isotope labeling experiments where some of the reaction products were not available for calibration, it was necessary to estimate the cracking pattern and the mass spectrometer sensitivity by one of two methods. The first method was used to calculate the partial pressure of C-13 labeled ethylene and ethane isotopes and involved two assumptions. The mass spectrometer sensitivity with respect to the total ion current contributed by a given species was considered to be the same for all C-13 isotopes. Moreover, cracking patterns were calculated from experimental $C_2^{12}H_4$ and $C_2^{12}H_6$ patterns by assuming that ionization probabilities did not change when C-12 was replaced by C-13.

The second method was used to determine partial pressures of deuteroethanes where the assumption of equal ionization probabilities for deuterium and hydrogen atoms bonded to carbon is not valid. Two sources in the literature (57, 58) gave cracking patterns for all ten deuteroethanes. These two sets of spectra were obtained in different labs under different sets of conditions and differ significantly. It was found, however, (after normalizing each cracking pattern to the same ion current) that a combination of 55% of one of these literature patterns for pure ethane, plus 45% of the other reproduced fairly accurately the ethane spectrum observed on the Quad 150 mass spectrometer, and it was therefore assumed that this combination would give a good spectrum for each deuteroethane. Again the assumption was made of equal mass spectrometer sensitivities with respect to the sum of the ion currents for each deuteroethane.

Once the cracking patterns and mass spectrometer sensitivities for all the species present in a mixture of gases produced in an experiment are measured or calculated, it is necessary to determine the combination of partial pressures which best reproduces the experimental spectrum. This procedure simply involves multiplication of an observed ion current at a given a.m.u. by the sensitivity, in the case where only one chemical species contributes to the intensity of that peak.

To illustrate the procedure when this is not the case, we consider the combination of C_2H_6, C_2H_5D, $CH_2D\text{-}CH_2D$ and $CHD_2\text{-}CH_3$ which results from dosing D_2 and C_2H_6 over the iridium film at $100^{\circ}C$. The most intense peaks in the cracking pattern of these species occur in the a.m.u. range 26-32 but there is considerable overlap. These cracking patterns (normalized to equal total ion current per unit pressure, as described above) are

designated $Im^{(1)}$, $Im^{(2)}$, $Im^{(3)}$ and $Im^{(4)}$ where m is the atomic mass unit (m = 26, 27 --- 32) and (1) refers to C_2H_6, (2) to C_2H_5D, etc. The experimental ion current at a given a.m.u. is designated im and Δim is defined as follows

$$\Delta im \equiv im - \left(Im^{(1)} U_1 + Im^{(2)} U_2 + Im^{(3)} U_3 + Im^{(4)} U_4\right)$$

where the mole fraction of, for example, C_2H_5D ($X^{(2)}$) is given by

$$X^{(2)} = \frac{U_2}{(U_1 + U_2 + U_3 + U_4)}$$

f is defined $f \equiv \sum_{m=26}^{32} \left(\frac{\Delta im}{im}\right)^2$ and the condition for best fit $\frac{\partial f}{\partial Un} = 0$ gives four equations in the four unknowns, Un (n = 1,2,3,4), the solution of which allows a determination of the partial pressure of each deuteroethane.

This method can, of course, be generalized and any number of superimposed spectra be separated in this way as long as the number of peaks in the experimental spectrum is equal to or greater than the number of isotopes (or other combination of gases present). This procedure, however, allows for negative Un values--if this occurs it suggests poor calculated cracking patterns, errors in the subtraction of background peaks or other random errors in an experimental spectrum, particularly if the concentration of one isotope is near zero.

The capacitance manometer (Granville-Phillips Co.) had a low pressure resolution of 5×10^{-5} torr and could measure pressures up to 1 torr. The head of the manometer consisted of a thin metal diaphragm (see Figure 5), one side of which was always maintained at pressures lower than 1×10^{-5} torr. Pressure on the other side of the diaphragm would cause a

displacement relative to a fixed probe and a change in capacitance. This change was transformed by the control unit to an A.C. electrical signal which was amplified and displayed. The major problem in the operation of the manometer was a large zero drift caused by variations in the temperature of the head. For this reason the head was wrapped with tubing through which water from a constant temperature bath was pumped.

The gases used in this study were research grade and in certain cases were further purified by vacuum distillation. In all cases their purity was verified by mass spectrometer analysis. The iridium wire (obtained from Engelhard Industries) was 99.9% pure.

The iridium single crystal was obtained from Materials Research Corporation as a quarter-inch rod. Its main impurity was specified to be 100 ppm Ru. The crystal orientation was determined by back reflection Laue x-ray diffraction following which several discs were spark cut from the rod and mechanically polished; the final polish involved .05 μ particle size (Linde B Alumina). The disc orientations following this procedure were found to be within 1^{o} of that desired.

RESULTS AND DISCUSSION

Ethylene Hydrogenation

As indicated in the literature review, a wide spectrum of possible Rideal-Eley and Langmuir-Hinshelwood type reaction mechanisms have been proposed to explain the ethylene hydrogenation. The purpose of the experiments described below was to discriminate among these possibilities over an iridium catalyst and under reaction conditions where surface dehydrogenation would not cloud the interpretation. All the ethylene hydrogenation results were obtained over iridium thin films in the thickness range 50 to 200^{o}A, deposited at 100^{o}C.

The field emission results of Arthur and Hansen (40) described earlier show a change in the surface electronic structure as characterized by work function changes at a temperature of $\sim$ 150 K. To test their interpretation that this change was caused by ethylene dehydrogenation on the surface, the following experiment was carried out.

A fresh iridium film was brought to 110 K and dosed with enough ethylene to produce a pressure of several microns. Over a time period of $\sim$ 1 hr., no ethane product was observed so the bath temperature was slowly raised at a rate of $\sim$ 0.02 deg/sec. At $\sim$ 145 K the first traces of ethane began to appear in the gas phase (the detection limit for ethane, $\sim$ 1 x 10^{15} molecules was in this case less than 1% of the ethylene molecules adsorbed on the film surface).

On the other hand, hydrogenation readily occurred upon addition of ethylene and hydrogen to a film at 110 K. These two results taken together support the interpretation of the field emission results and suggest that

either gas phase or adsorbed hydrogen is necessary for hydrogenation to occur, thus eliminating from consideration the self-hydrogenation mechanisms involving two adsorbed or one adsorbed and one gas phase ethylene molecule.

Ethylene adsorbed very strongly on the iridium films. For example, if small doses of ethylene were sequentially added to a fresh film at 150 K, no gas phase ethylene could be detected until the film was nearly saturated. Because of this strong adsorption and because of the high surface to volume ratio in the reaction chamber, the number of ethylene hydrogenation sites could be counted. This number was found to be less than the total number of adsorbed ethylene molecules and was determined at 150 K by the following procedure.

First, slightly more than a saturation dose of C-13 labeled ethylene was added to a clean film. Immediately following this H_2 and $^{12}C_2H_4$ were added and the production of $^{13}C_2H_6$ monitored until no further increase was observed. The number of adsorbed ethylene molecules can readily be calculated from the known manifold and reaction cell volumes and the difference in capacitance manometer pressures before and after the initial dose. Of the labeled ethylene initially adsorbed, $\sim$ 54% remained on the film surface, the remainder desorbed as ethane. The number of hydrogenation sites (defined as the number of initially adsorbed $^{13}C_2H_4$ molecules which eventually appeared in the gas phase as ethane) for the 300 cm^2 of surface area was 2 x 10^{17} sites/100 A^o of film thickness.

The temperature dependence of the hydrogenation reaction rate is shown in Figure 7 in the form of an Arrhenius plot which is linear up to a temperature of $\sim$ 200 K. Above 200 K the rate drops rapidly with increasing

Figure 7. Arrhenius plot for 123 μ H_2 and 79 μ C_2H_4 reacting over a 100 A° Ir film between 150 and 205 K (the rate has dimensions molecules/sec). As the bath temperature was raised over 200 K, the rate of ethane production fell rapidly toward zero. However, if the bath temperature was subsequently set at 150 K and the concentrations of reactants set at their original values, the initial rate was reproduced within experimental error. The reduction in catalytic activity above $\sim$ 200 K is attributed to a surface dehydrogenation with a resulting decrease in the concentration of surface intermediates for the hydrogenation reaction. Over the linear portion of the curve, however, the rate of the interfering dehydrogenation reaction ((f) step 7) is negligible

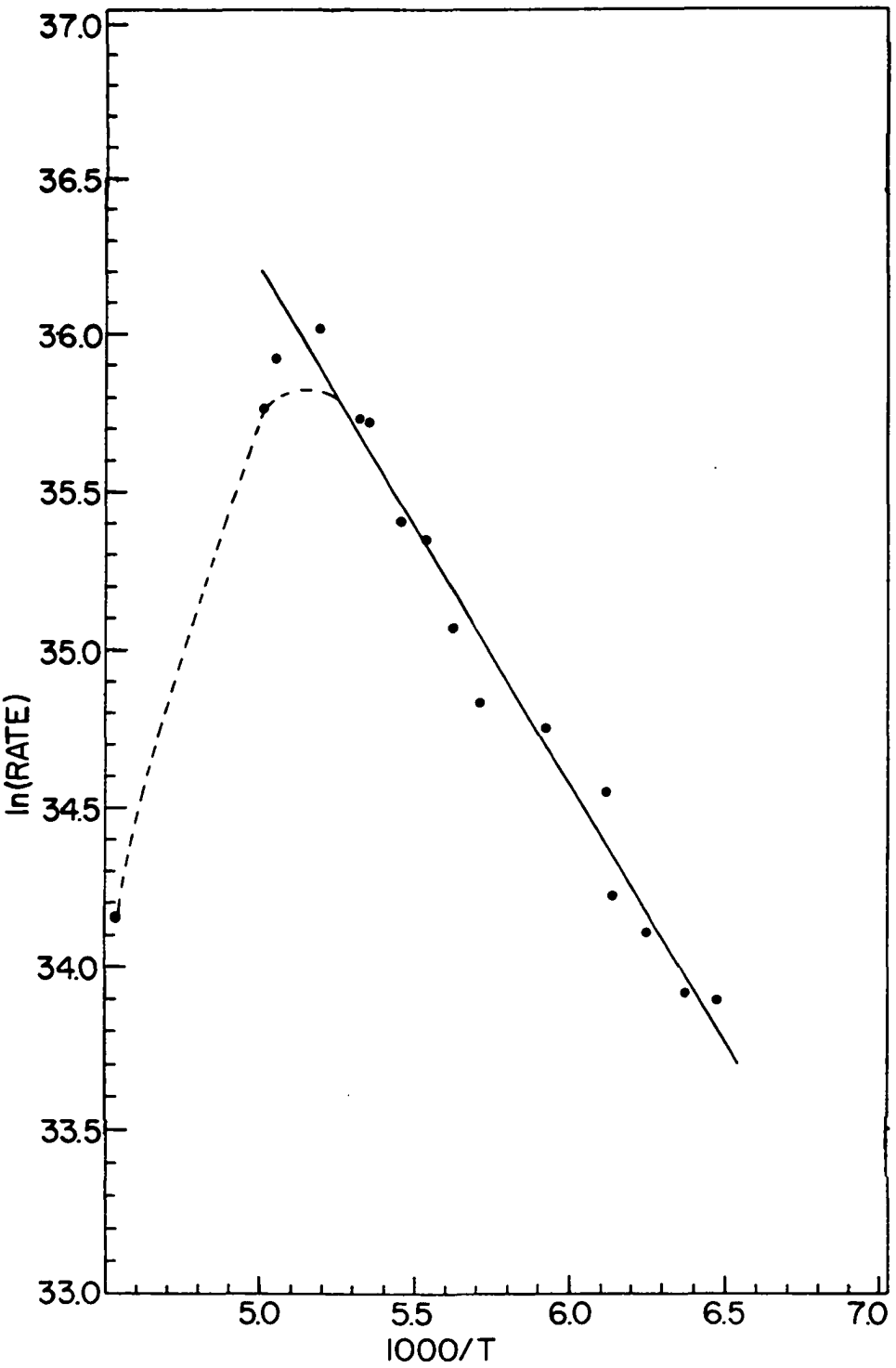
37.0
36.5
36.0
35.5
35.0
34.5
34.0
33.5
33.0
ln(RATE)
5.0
5.5
6.0
6.5
7.0
1000/T

temperature, but over the temperature range of Figure 7, this drop in rate can be reversed by restoring a lower temperature. That this decrease in rate is caused by surface dehydrogenation of a hydrocarbon species adsorbed on the hydrogenation sites is shown by substitution of C_2D_4 for C_2H_4 in the experiment described above. As the temperature is reached at which the Arrhenius plot becomes nonlinear, there is a sharp increase in the concentration of H-D and D_2 in the gas phase which can only be caused by the dehydrogenation of adsorbed species. The dependence of the rate on the partial pressures of hydrogen and ethylene was investigated at 110 K. As shown in Figure 8, the reaction was 1/2 order in hydrogen pressure and zeroth order in ethylene pressure. Results of experiments of the type shown in Figures 7 and 8 give a rate law which applies only under conditions of negligible dehydrogenation on the hydrogenation sites.

$$R = k\,[C_2H_4(g)]^{\,o}\,[H_2(g)]^{1/2}\,\exp\left(\frac{-3.3\ \text{kcal}}{RT}\right)$$

Moreover at 110 K and 150 K the major deuteroethane produced (> 95%) when D_2 is substituted for H_2 during the steady state hydrogenation is $C_2H_4D_2$. However, if instead of dosing C_2H_4 and D_2 simultaneously, the iridium film is first dosed with D_2 followed by a slow (e.g. 10^{17} molec/sec) dose of ethylene, then there is a much wider spread in the deuteroethane product distribution, with a substantial fraction of the initial ethane product appearing as C_2D_6.

All these experiments are consistent with a Horiuti-Polanyi type hydrogenation mechanism with several modifications. In the first place, since ethylene adsorbs strongly on the iridium films and since the order in ethylene pressure is never observed to be less than zero, it is not

Figure 8. Plot showing the zeroth order dependence of the rate on ethylene pressure and the 1/2 order in hydrogen at 110 K. The pressure of ethylene was 22.6 μ at all points on the graph except for F where the ethylene pressure was 125 μ. At this temperature surface dehydrogenation of ethylene is negligible and the observed orders are consistent with a modified Horiuti-Polanyi hydrogenation mechanism

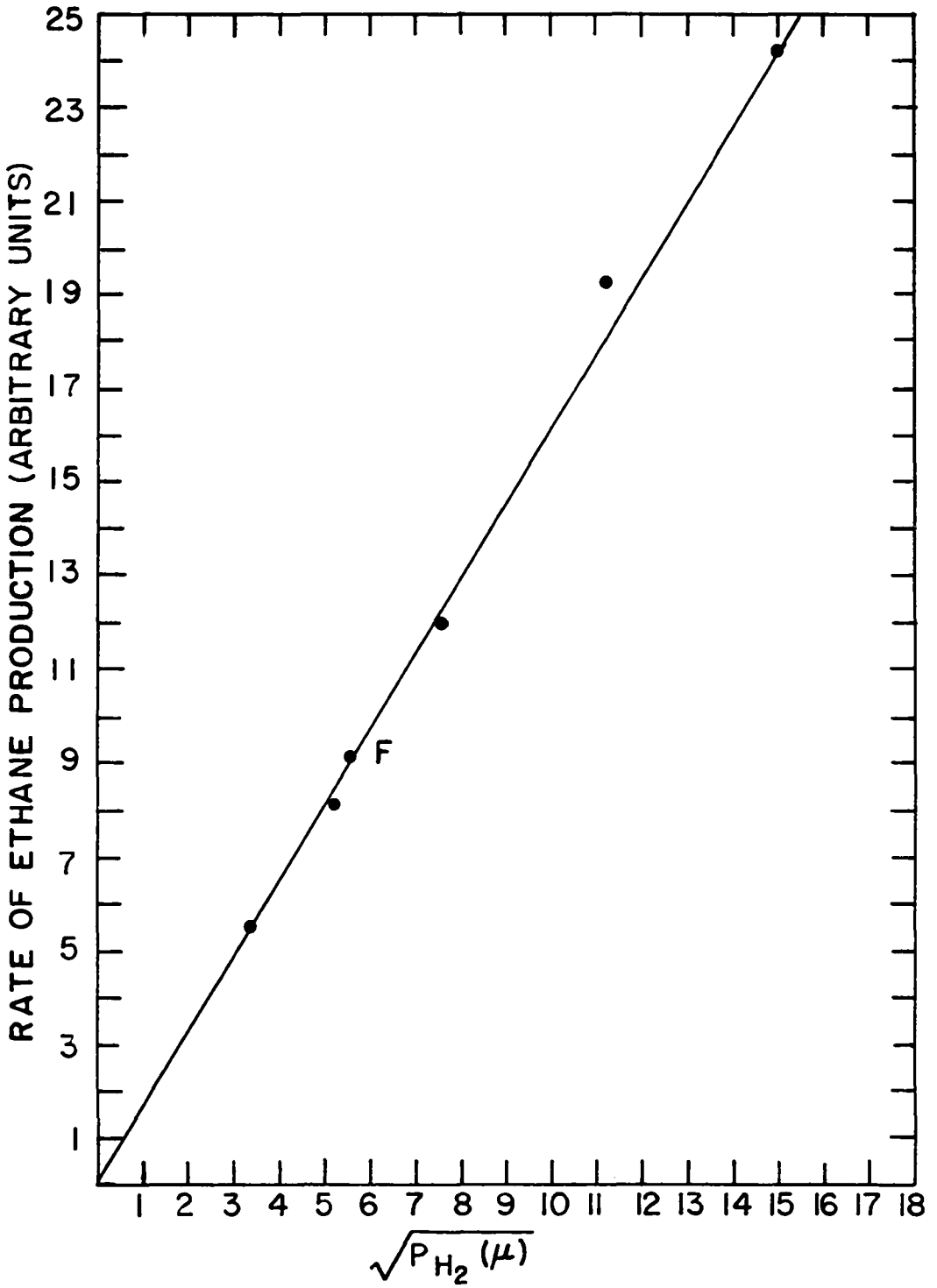
RATE OF ETHANE PRODUCTION (ARBITRARY UNITS)
25
23
21
19
17
15
13
11
9
7
5
3
1
F
1 2 3 4 5 6 7 8 9 10 11 12 13 14 15 16 17 18
$\sqrt{P_{H_2}(\mu)}$

unreasonable to assume that hydrogen does not compete for the sites on which ethylene is adsorbed but adsorbs on other sites. The sites on which the ethylene involved in hydrogenation adsorbs are designated by * and the sites where hydrogen adsorbs as *′. Secondly, to take into account the part of the surface that is not active for hydrogenation we must designate yet another type of site for even stronger ethylene adsorption $\overset{*}{\downarrow}$. The proposed steps are

1. $H_2(g) + 2\,*' \underset{k_{-1}}{\overset{k_1}{\rightleftharpoons}} 2\,\underset{*'}{H}$

2. $C_2H_4(g) + 2\,* \underset{k_{-2}}{\overset{k_2}{\rightleftharpoons}} \underset{*}{CH_2} - \underset{*}{CH_2}$

3. $\underset{*}{CH_2} - \underset{*}{CH_2} + \underset{*'}{H} \underset{k_{-3}}{\overset{k_3}{\rightleftharpoons}} \underset{*}{CH_2} - CH_3 + *' + *$

4. $\underset{*}{CH_2} - CH_3 + \underset{*'}{H} \underset{k_{-4}}{\overset{k_4}{\rightleftharpoons}} C_2H_6(g) + *' + *$

5. $C_2H_4(g) + 2\,\overset{*}{\downarrow} \underset{k_{-5}}{\overset{k_5}{\rightleftharpoons}} \underset{\overset{*}{\downarrow}}{CH_2} - \underset{\overset{*}{\downarrow}}{CH_2}$

6. $\underset{*}{CH_2} - \underset{*}{CH_2} \underset{k_{-6}}{\overset{k_6}{\rightleftharpoons}} \underset{*}{CH} = \underset{*}{CH} + H_2(g)$

7. $\underset{\overset{*}{\downarrow}}{CH_2} - \underset{\overset{*}{\downarrow}}{CH_2} \underset{k_{-7}}{\overset{k_7}{\rightleftharpoons}} \underset{\overset{*}{\downarrow}}{CH} = \underset{\overset{*}{\downarrow}}{CH} + H_2(g)$ (f)

The only steps of concern in the steady state hydrogenation kinetics over the temperature range where the Arrhenius plots are linear are 1 through 4. The maxima in the Arrhenius plots occur near the point at

which the rate of the foreward reaction of step 6 becomes significant enough to influence the overall rate. Step 5 accounts for the irreversibly adsorbed carbon left on the surface (with $k_{-5} = 0$), and since the resulting surface species is probably more strongly adsorbed than $\underset{*}{CH_2} - \underset{*}{CH_2}$, it is likely that the first traces of self-hydrogenation observed upon heating the saturated film of ethylene from 110 K are due to the production of hydrogen caused by the occurrence of step 7 in the forward direction.

The kinetic consequences of a Horiuti-Polanyi mechanism formally similar to steps 1 through 4 have been derived (59). If it is assumed $k_4 >> k_{-4}$ and if the steady state approximation is used to derive an expression for $\underset{*}{CH_2} - CH_3$, we obtain a rate law of the form,

$$\frac{d[C_2H_6]}{dt} = k_4 \left[\underset{*}{CH_2} - CH_3\right] \left[\underset{*'}{H}\right]$$

$$= \frac{k_4 k_3 \left[\underset{*'}{H}\right]^2 \left[\underset{*}{CH_2} - \underset{*}{CH_2}\right]}{k_{-3} [*] [*'] + k_4 \left[\underset{*'}{H}\right]} \qquad (g)$$

If $k_{-3} [*] [*'] << k_4 \left[\underset{*}{H}\right]$

$$\frac{d [C_2H_6]}{dt} = k_3 \left[\underset{*'}{H}\right] \left[\underset{*}{CH_2} - \underset{*}{CH_2}\right]$$

$$= k [H_2]^{1/2} [C_2H_4]^{0} \qquad (h)$$

as observed, if the adsorption isotherm describing the surface concentration of $\underset{*'}{H}$ has the same behavior as the Langmuir isotherm for dissociative diatomic adsorption in the low pressure limit and if the isotherm expression for $\underset{*}{CH_2} - \underset{*}{CH_2}$ saturates the unprimed sites over our pressure range. When $k_{-3} [*] [*'] << k_4 \left[\underset{*'}{H}\right]$ nearly every $\underset{*}{CH_2} - CH_3$ species formed will

go on to form ethane, and substitution of deuterium for hydrogen will result in the production of primarily $C_2H_4D_2$ as observed. On the other hand, when ethylene is slowly dosed onto the deuterium predosed surface, [*] is initially large enough that the k_{-3} [*] [*'] term in the denominator of (g) is no longer negligible. The reverse of reaction 3 can now take place at a rate comparable to step 4, which results in the observed spread of deutero-ethane products.

Equations (g) and (h) only apply, of course, when the reaction conditions of temperature and pressure are such that the rate of surface dehydrogenation of ethylene adsorbed on the catalytically active sites is negligible. At higher temperatures it is assumed from the field emission (40) and thermal desorption (41) results described earlier that the dehydrogenation, under conditions where the surface is nearly saturated with ethylene, produces adsorbed acetylene and gaseous hydrogen as in step 6. In order to test the validity of this assumption, ethylene self-hydrogenation results obtained by P. Masterson (2) at 100°C over identically prepared iridium films were fit to a rate law derived from these steps. In this experiment Masterson had dosed enough ethylene to saturate the film and leave several microns in the gas phase. The ethane pressure was monitored and is shown as the x's in Figure 9. The ethane production is initially very rapid but soon falls off to zero as the surface is poisoned by dehydrogenated ethylene species and as the hydrogen supply from this surface dehydrogenation reaction is depleted.

This self-hydrogenation is modeled as follows (the concentration symbols [ ] in this case are taken to refer to the unit volume and unit area consisting of the total reaction volume and the total surface area of the

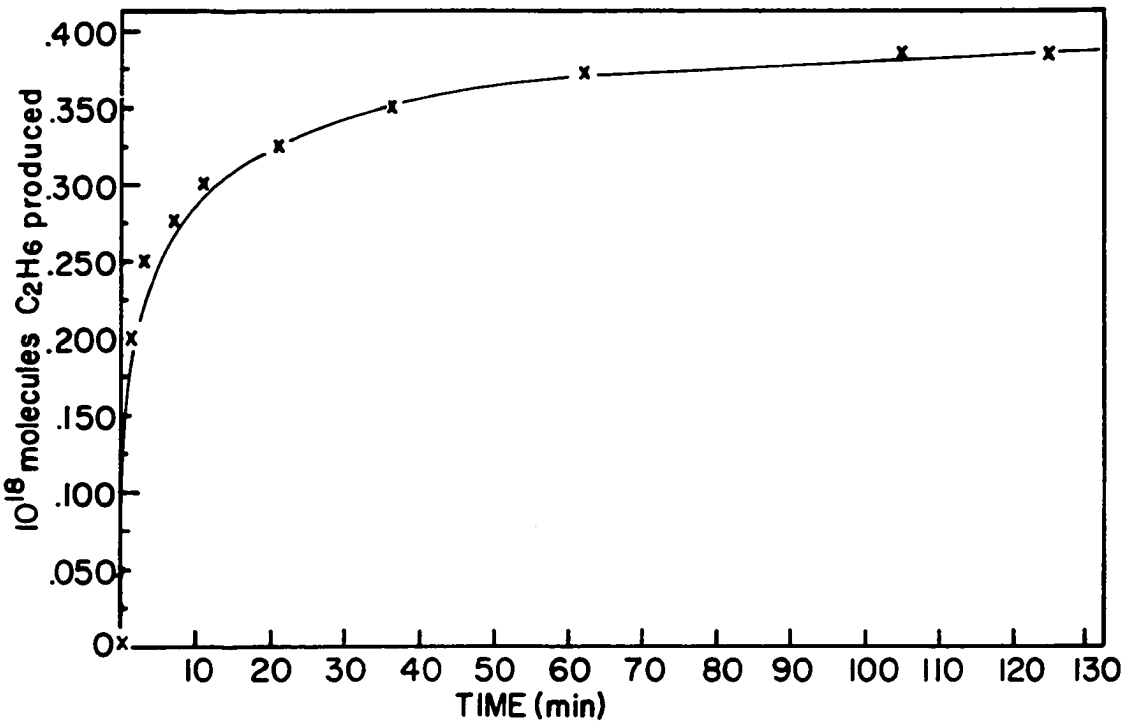

Figure 9. Plot showing the total number of ethane molecules produced in time when an excess of ethylene (but no hydrogen) was dosed over a bare 100 A^{o} Ir film at 100°C. The x's are experimental points and the solid line is obtained by numerical integration of (k). No methane was produced

catalyst). Steps 6 and 7 are taken to be irreversible under the reaction conditions (100°C and low hydrogen pressure) so that

$$\frac{d\left[\begin{matrix}CH = CH\\ * \quad *\end{matrix}\right]}{dt} = k_6 \left[\begin{matrix}CH_2 - CH_2\\ * \quad *\end{matrix}\right]$$

$$= k_6 \left(No - \left[\begin{matrix}CH = CH\\ * \quad *\end{matrix}\right]\right)$$

$$\left[\begin{matrix}CH_2 - CH_2\\ * \quad *\end{matrix}\right] = No - \left[\begin{matrix}CH = CH\\ * \quad *\end{matrix}\right]$$

$$= No \exp(-k_6 t) \qquad (i)$$

where $$\left[\begin{matrix}CH_2 - CH_2\\ * \quad *\end{matrix}\right] + \left[\begin{matrix}CH = CH\\ * \quad *\end{matrix}\right] = No$$

where No is a constant, the total number of active sites.

In the same way

$$\left[\begin{matrix}CH_2 - CH_2\\ *\downarrow \quad *\downarrow\end{matrix}\right] = Uo - \left[\begin{matrix}CH = CH\\ *\downarrow \quad *\downarrow\end{matrix}\right] = Uo \exp(-k_7 t) \qquad (j)$$

Substitution of (i) into (h) gives

$$\frac{d[C_2H_6]}{dt} = k_3 \left[\begin{matrix}H\\ *'\end{matrix}\right] No \exp(-k_6 t)$$

The rate law (h) is derived by assuming that the surface concentration of hydrogen atoms is given by an isotherm which has the same behavior as the Langmuir isotherm for dissociative diatomic adsorption in the low pressure limit. This suggests that we can assume that the concentration of adsorbed hydrogen atoms is close to zero and given by $\left(\frac{k_1}{k_{-1}}\right)^{1/2} (H_2)^{1/2}$ with

$$[H_2(g)] = \left[\begin{matrix}CH = CH\\ * \quad *\end{matrix}\right] + \left[\begin{matrix}CH = CH\\ *\downarrow \quad *\downarrow\end{matrix}\right] - [C_2H_6(g)]$$

$$= No - No \exp(-k_6 t) + Uo - Uo \exp(-k_7 t) - [C_2H_6(g)]$$

since in this experiment no hydrogen was dosed, so that

$$\frac{d\,[C_2H_6]}{dt} = k_3 \left(\frac{k_1}{k_{-1}}\right)^{1/2} No\,[H_2(g)]^{1/2} \exp(-k_6 t)$$

$$= k_3 \left(\frac{k_1}{k_{-1}}\right)^{1/2} No \exp(-k_6 t)\,[No - No \exp(-k_6 t)$$

$$+ Uo - Uo \exp(-k_7 t) - [C_2H_6(g)]]^{1/2} \qquad (k)$$

Equation (k) was numerically integrated and the fit to experiment, shown as the solid line in Figure 9, was obtained by freely varying the values of t the constants No, Uo, k_6, k_7 and $k_3\left(\frac{k_1}{k_{-1}}\right)^{1/2}$. These values were found to be 1.6×10^{17} sites, 2.30×10^{17} sites, 0.040 min^{-1}, 13.0 min^{-1}, and 3.60×10^{-9} $molec^{-1/2}$ min^{-1}, respectively. The site densities No and Uo and the ratio No/(Uo + No) found in this way (for the $\sim$ 100 A^{o} film of Figure 3) compare favorably with values obtained at 150 K using C-13 labeled ethylene, as discussed above. The fact that $k_3\left(\frac{k_1}{k_{-1}}\right)^{1/2}$ is found to be as small as 3.60×10^{-9} is consistent with the assumption made in the development of this model, that the concentration of adsorbed hydrogen is close to zero (from which $k_{-1} >> k_1$). The shape of the curve is fairly sensitive to small changes in the values of all constants except k_7. Because of the experimental scatter, the only thing we can say with confidence about the value of k_7 is that it is many times larger than k_6.

Masterson had shown that a slow ($\sim 5 \times 10^{14}$ molec/sec) dose of ethylene onto either a bare or hydrogen predosed Ir film ($\sim$ 100 A^{o} thick, 100°C) produced methane as the major product and smaller amounts of ethane and hydrogen. Comparing these experiments with Figure 9, where all the

ethylene is dosed at once and no CH_4 produced, suggests that the mechanism of methane formation from ethylene involves $C_2H_6(g)$ as an intermediate. For heavy ethylene doses as in Figure 9, the sites where ethane might readsorb are blocked by ethylene or its dehydrogenation products and thus no methane is produced.

However, the dehydrogenation products resulting from reactions (f) steps 6 and 7 look remarkably like the di-sigma bonded $C_2H_2(a)$ species proposed by Sinfelt (45, 48, 60) as the intermediate in the ethane hydrogenolysis reaction over Ir. If it were the case that these surface species were the same, addition of ethylene should not poison the hydrogenolysis reaction, but in fact at 100°C it does.

In order to resolve this discrepancy, the ethane hydrogenolysis reaction was investigated in detail. The results of this investigation are described in the following pages.

Ethane Hydrogenolysis

As demonstrated by Roberts (15, 61) and later Masterson (2), addition of only ethane ($\sim 10^{18}$ molecules) to a clean iridium film (~ 100 A° thick and ~ 300 cm^2 macroscopic surface area) results in an initial rapid production of gas phase hydrogen and a slower methane production which eventually depletes the hydrogen supply. The time period in which a significant fraction of the ethane reacts to form methane is several hours at a film temperature of 25°C but only several minutes at 100°C. Neither of these authors, however, carried out a systematic investigation of the dependence of the hydrogenolysis rate on the temperature or partial pressures of ethane, methane and hydrogen. One of the primary objectives of the work

described below was to carry out such an investigation and in particular to cover a range of partial pressures wide enough to allow for an adequate test of a proposed rate law.

The iridium single crystal surfaces were found to be considerably less active than was originally anticipated. The single crystal results are included near the end of this section; otherwise all the experimental results refer to reactions taking place over the polycrystalline thin film catalysts.

Preliminary kinetic results and the problem of irreproducibility

The first few experiments were carried out at film temperatures of 100°C over thin films which had been deposited at 100°C, and several features of the reaction immediately became obvious. In the first place, if the hydrogenolysis rate R (hereafter $R \equiv -\frac{d\ C_2H_6}{dt}$) was fit to a power rate law of the form $R = K\ P^n_{C_2H_6}\ P^m_{H_2}$, n and m were not constants for all partial pressures of hydrogen and ethane--instead the values of the exponents depended on these partial pressures. At very low partial pressures of either ethane or hydrogen, the reaction order was positive for each reactant. However, when the partial pressure of a given reactant was increased (while the partial pressure of the other reactant was held constant), the order in that reactant decreased, eventually became zero and then negative. The partial pressure range covered in these experiments was typically 2-3 orders of magnitude for each reactant.

These observations were at first difficult to describe quantitatively because of large amounts of scatter in the data. The magnitude of this scatter was considerably greater than that caused by instrumental noise.

It soon became apparent that at least two main factors were responsible for this irreproducibility, both of which were due to peculiarities of the thin film-ethane-hydrogen system. The effect of both of these factors, however, could be minimized by changes in the experimental procedure.

The first experiments had typically been carried out in the following way. A film would be deposited in vacuum at 100°C following which several microns of each reactant would be simultaneously introduced to the reaction cell. The dosing procedures and methods of measuring pressures have been described earlier. After a significant fraction of the reactants had been converted to methane (typically this required several hundred seconds), the cell would be pumped until the manometer pressure returned to zero. Reactants would then again be introduced to the reaction chamber and the process repeated, holding the partial pressure of one reactant constant while varying the pressure of the other reactant. Typically two sequential series of runs would be carried out; in each series a constant number of molecules of one reactant would be introduced in each run.

The first factor, which caused part of the experimental scatter, can be described as a "memory" characteristic of the film. For example, if a sequential series of runs at some standard conditions of ethane and hydrogen pressure was interrupted by insertion of a run with a much higher ethane pressure, the rate of hydrogenolysis in the runs immediately following the high pressure run would be less than expected. Generally, after two or three runs at the standard conditions the rate would return to the value it had prior to the high ethane pressure dose. With less extreme pressure changes from run to run, this effect would show up as small deviations from steady state conditions (i.e., the rate of methane production

would not be equal to two times the rate of ethane depletion from the gas phase) over the first part of the following run.

This problem was solved when it was discovered that this "memory effect" was due to adsorbed hydrocarbon species which remained on the surface when the cell was evacuated and prevented the rapid establishment of steady state conditions in the immediately following experiments. The experimental procedure was, therefore, changed and several microns of hydrogen were introduced to the reaction chamber after every hydrogenolysis run for several hundred seconds or until no further carbon appeared in the gas phase. This resulted in a considerable reduction of the experimental scatter.

As indicated in the literature review, a number of authors (43, 46) had studied the hydrogenolysis kinetics over a very limited range of partial pressures and in all cases had used an excess of hydrogen in order to avoid poisoning caused by carbon accumulation on the surface. One recent investigation (62) of hydrogenolysis over iron films goes so far as to conclude that ". . . extraction of kinetic information other than at zero time, would be of little value . . ." primarily because of this effect. The "memory effect," however, can easily be erased by slight procedural modifications and, as described shortly, this effect is an expected consequence of our proposed hydrogenolysis mechanism.

The second major cause of the scatter in the kinetic data was a slow, temperature dependent, irreversible change in the catalytic activity with time. The reason for this change was thought to be a structural change in the film surface, probably due to sintering (transformation of a number of small metal atom clusters into one larger cluster) with a corresponding

change in the distribution of the thermodynamic properties of the catalytically active sites.

Support for this interpretation as opposed to another explanation such as poisoning of the active sites by side reactions or impurities comes from the experiments summarized in the Arrhenius plots of Figures 10 and 11.

All of the data points in Figure 10, except for the three represented by the symbol +, represent hydrogenolysis rates obtained over a single iridium film which was deposited at a bath temperature of 100°C. These points were obtained by the following experimental procedure. Immediately after deposition of the film, $\sim$ 100 μ of a 50:50 hydrogen ethane mixture was allowed to expand from the manifold into the reaction cell which was still at the film deposition temperature ($1{,}000/T_B \sim 2.68$) whereupon the rate of hydrogenolysis was measured. The cell was then evacuated and the procedure repeated at a higher bath temperature. The temperature of the bath was raised in steps to 224°C ($1{,}000/T_B \sim 2.01$) at which point the temperature was lowered in steps. The x's represent a set of runs carried out over the same film on the following day with the time sequence, highest to lowest temperature. The runs represented by the symbol + were carried out over another film at a somewhat higher hydrogen to ethane ratio and are normalized in such a way that the value of R at 100°C is equal for the two films represented in Figure 10. The hydrocarbon residue was not removed by hydrogenation for any of the runs represented in Figure 10. This is not, however, expected to affect the results since a constant ratio of hydrogen to ethane was introduced to the reaction chamber each run.

The decrease in film activity which causes the maximum in the Arrhenius plot is irreversible. This fact taken in conjunction with the

Figure 10. The temperature dependence of the hydrogenolysis rate is shown for two thin film catalysts each prepared at a bath temperature of 100°C. For the first film the rates are represented by the symbol + and the bath temperature is not raised above 100°C ($1{,}000/T_B \sim 2.68$). The hydrogenolysis rates over the second film are represented by •'s and x's. The first run over this film is carried out at 100°C, then the bath temperature is increased in steps and the hydrogenolysis rate is observed to pass through a maximum. After reaching the highest bath temperature of this figure ($T_B \sim 224$, $1{,}000/T_B \sim 2.01$), the bath temperature is lowered in steps. The x's represent a series of runs carried out over this film on the following day. The decrease in film activity caused by the high bath temperature is irreversible. The apparent activation energy corresponding to the slope of the two lines drawn through the data points is 25.5 kcal/mole

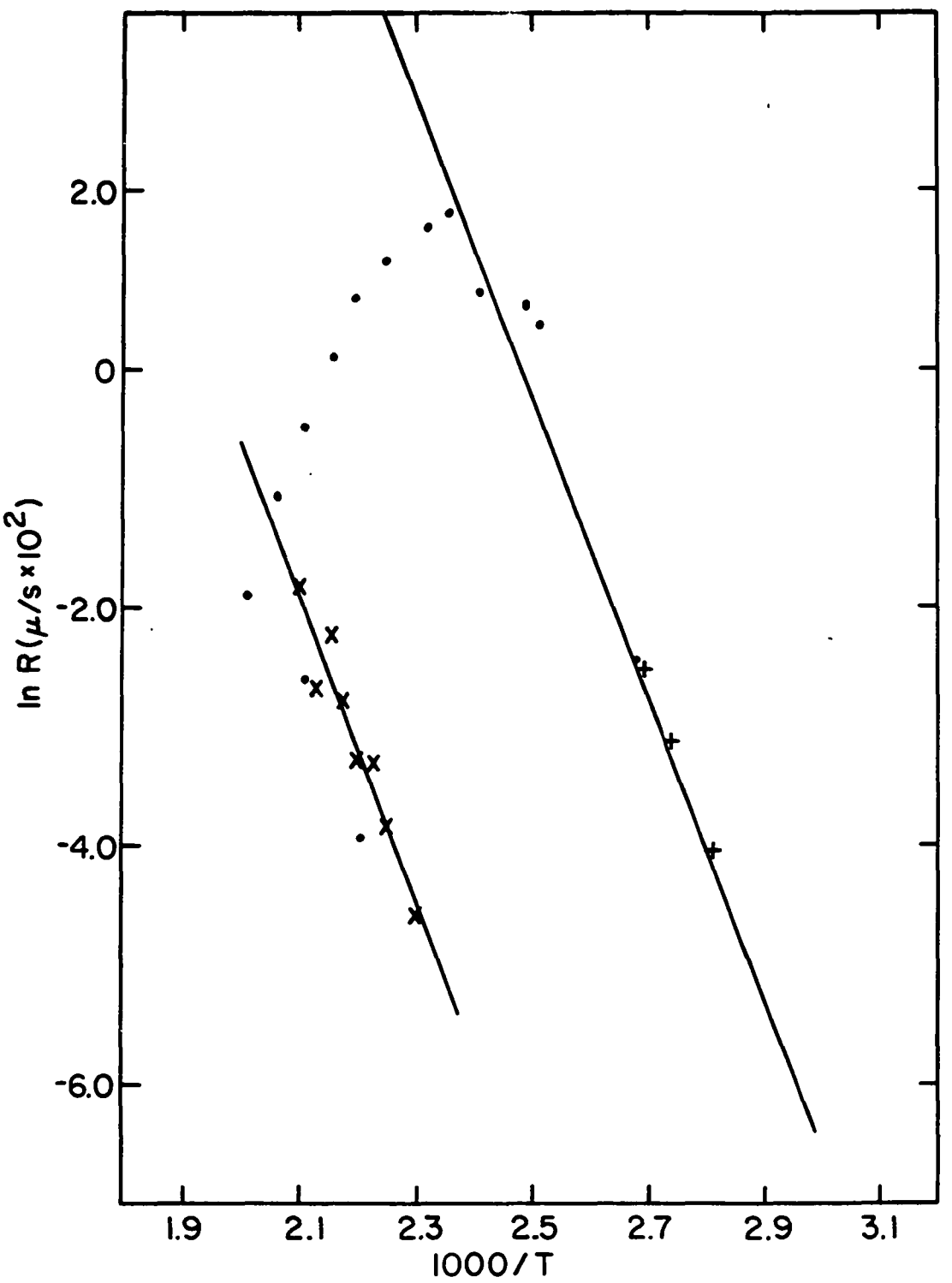
2.0
0
-2.0
-4.0
-6.0
ln R(μ/s x 10²)
1.9
2.1
2.3
2.5
2.7
2.9
3.1
1000/T

Figure 11. The temperature dependence of the hydrogenolysis rate is shown for an iridium film deposited at 225°C. The time sequence of runs is lowest to highest temperature. No rate maximum is observed in this case although the same range of temperatures is covered as in Figure 10. The apparent activation energy over the linear portion of this curve is $\sim$ 19.6 kcal/mole suggesting that there are significant differences in the properties of well annealed and partially annealed thin films

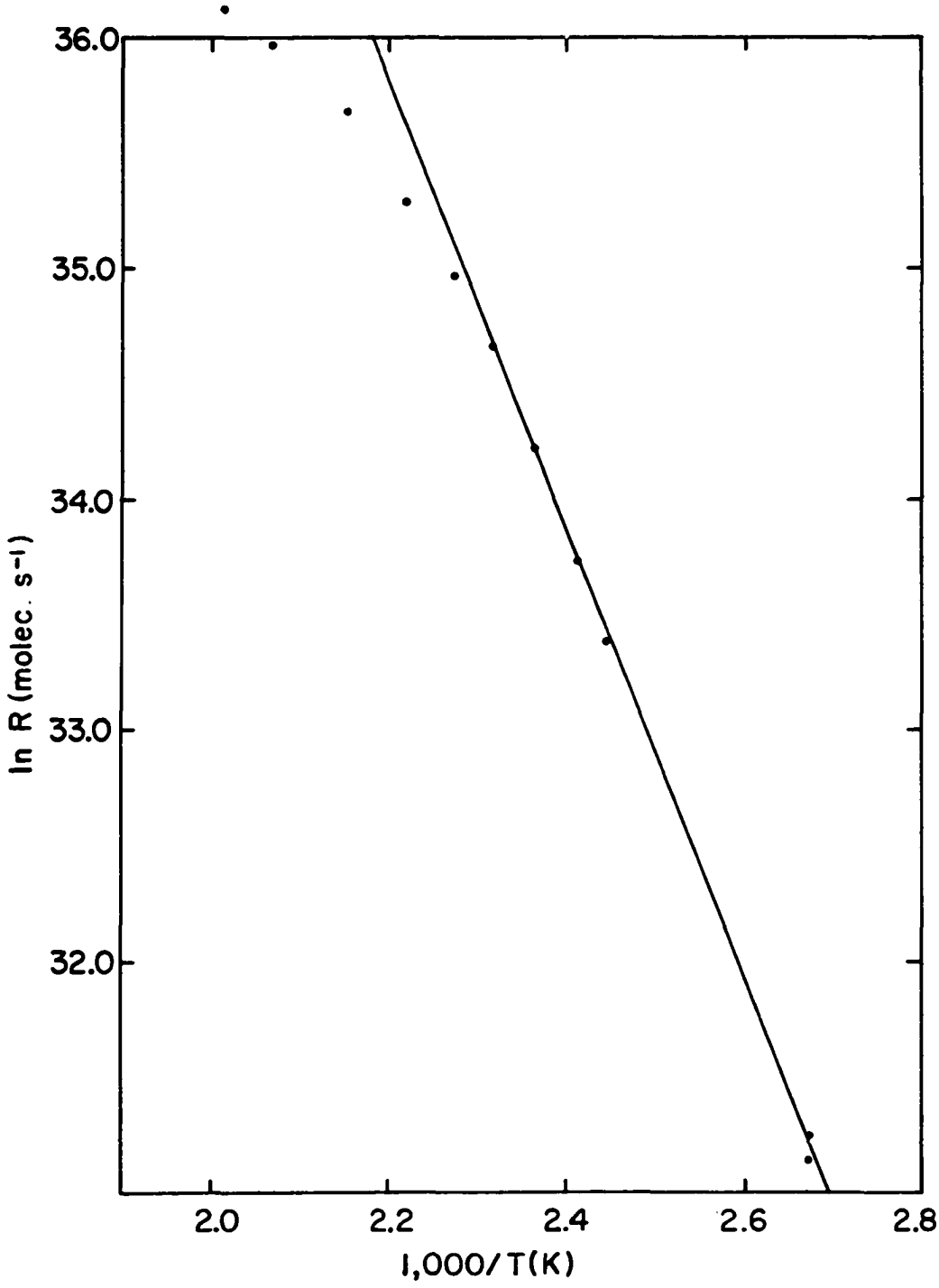
36.0
35.0
34.0
33.0
32.0
ln R (molec. s⁻¹)
2.0
2.2
2.4
2.6
2.8
1,000/T(K)

observation that the slopes of the two lines in Figure 10 drawn through the somewhat scattered data points are approximately equal suggests that the same elementary steps are important in both cases and that the primary difference in rate is a difference in the number of active sites.

In order to further test the interpretation that the decrease in activity is caused by sintering, the film of Figure 11 was deposited at 225°C, then brought to 100°C where the hydrogenolysis rate was measured and the bath temperature raised in steps as in Figure 10. It is to be expected that the extent of sintering during film deposition at 225°C would be considerably greater than at 100°C, and indeed in this case the deviation from the linearity of the Arrhenius plot is much less pronounced than in Figure 10.

The consequences of the sintering for the kinetic analysis were particularly pronounced for runs carried out at 100°C over films deposited at 100°C. Under these circumstances a considerable amount of sintering took place during the course of the hydrogenolysis rate measurements, and it was necessary to return to some standard conditions of reactant partial pressures every few runs. All the observed rates would then be adjusted to the values they would have had, had no decrease in the hydrogenolysis rate with time at the standard conditions taken place. This correction was much smaller when films were deposited and runs carried out at temperatures near 200°C, as much of the sintering took place during film deposition. The effects of sintering on the analysis could be reduced even further by depositing the film at a bath temperature somewhat higher than the intended reaction temperature.

Hydrogenolysis rate measurements

Figures 12 and 13 show the dependence of the rate on the partial pressure of each reactant at a film temperature of 100°C. These data are expressed as the log of the rate (corrected for the decrease in activity caused by sintering) vs. the log of the pressure of one reactant (the pressure of the other reactant being approximately constant for each figure). After every run the cell was evacuated, then flushed with hydrogen as described above.

The solid line in each figure shows the fit to a rate law of the form

$$R = \frac{(C_2H_6)}{\left(a + b\,\frac{(C_2H_6)}{(H_2)^{1/2}} + c\,\frac{(C_2H_6)}{(H_2)} + d\,(H_2)^{1/2} \right)^2} \qquad (1)$$

where a, b, c and d are constants whose values are given in the figure captions. In these log-log plots, the slope is the order with respect to a power rate law.

The results of a similar experiment on another film at somewhat higher reactant pressures are shown in Figures 14 and 15. In these figures the rate is expressed in dimensions molec. s^{-1} cm^{-2}. The conversion from μ to molec. s^{-1} cm^{-2} requires a knowledge of the surface area of active sites and is described later. It should be noted that the constants in the fit to equation (1) of Figures 14 and 15 are not exactly the same for the two series of runs. This is thought to be a consequence of the change in surface structure with time due to sintering. The two series of runs, in this case, can be viewed as two sets of experiments carried out on two catalysts of slightly different structures.

Figure 12. The dependence of the rate on the partial pressure of ethane at 100°C is shown for a thin film deposited at 100°C. The experimentally measured hydrogenolysis rates were corrected for a slow irreversible poisoning as discussed in the text. The solid line is the fit to equation (1) when the values of the four constants are $a = 0.148\ s^{1/2}$, $b = 0.268\ s^{1/2}\ \mu^{1/2}$, $c = 0.0\ s^{1/2}$ and $d = 0.145\ s^{1/2}\ \mu^{1/2}$. This kinetic behavior immediately suggests that ethane and hydrogen compete for the same sites

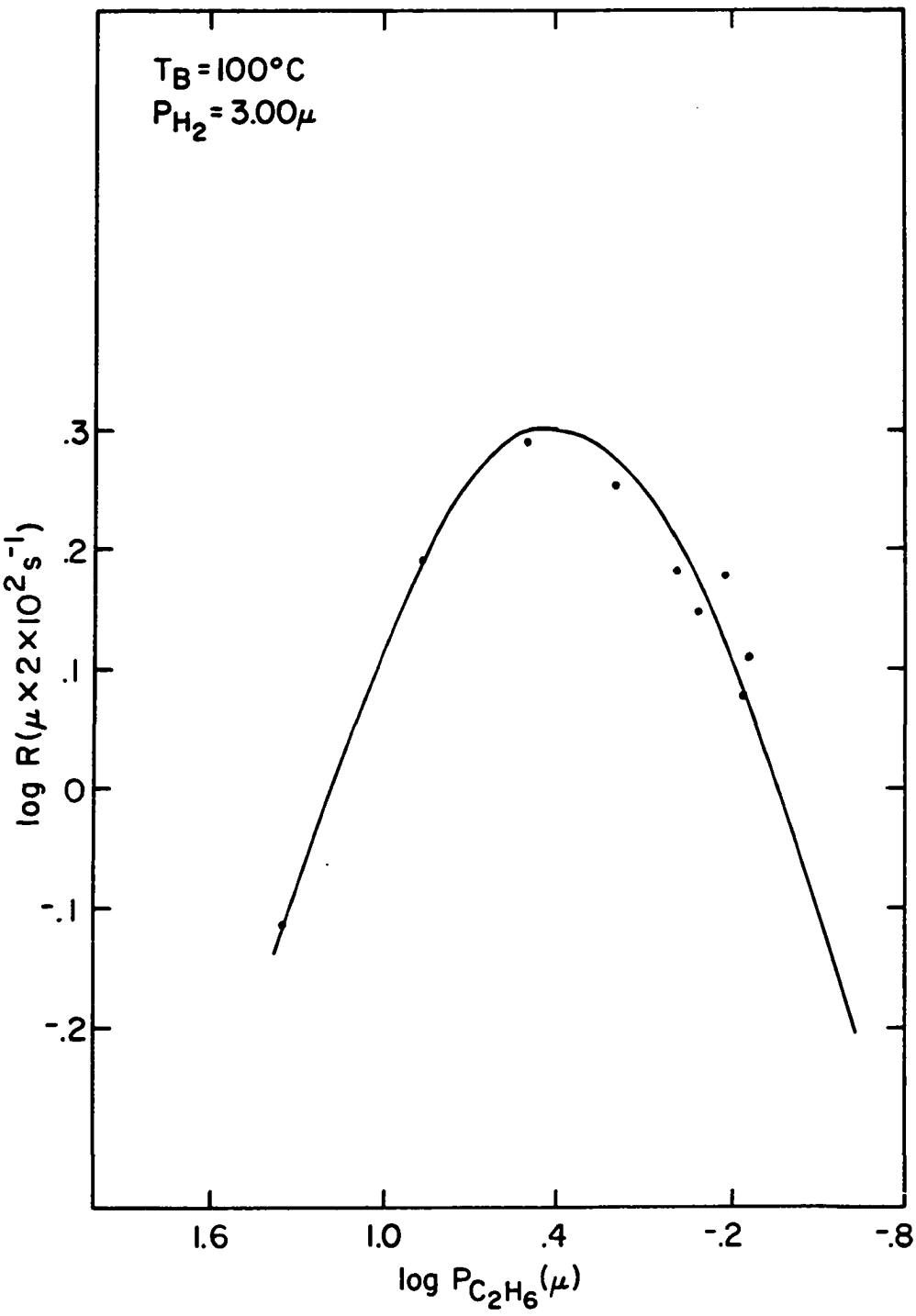
$T_B = 100°C$
$P_{H_2} = 3.00\mu$
log $R(\mu \times 2 \times 10^2 s^{-1})$
.3
.2
.1
0
-.1
-.2
1.6
1.0
.4
-.2
-.8
log $P_{C_2H_6}(\mu)$

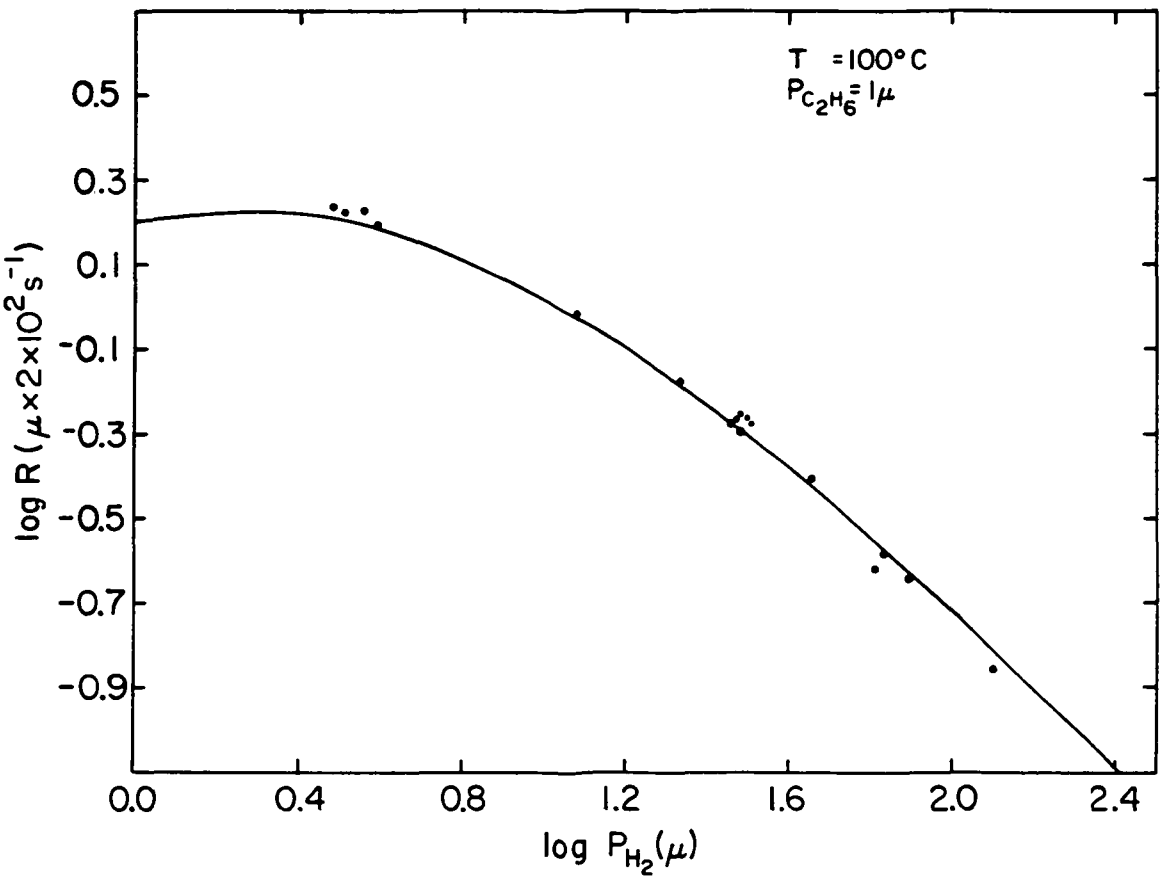

Figure 13. These data are taken over the same film as in Figure 12 and show the dependence of the hydrogenolysis rate on the pressure of hydrogen. The solid line is the fit to equation (1) where the constants a, b, c and d have the same values as in Figure 12

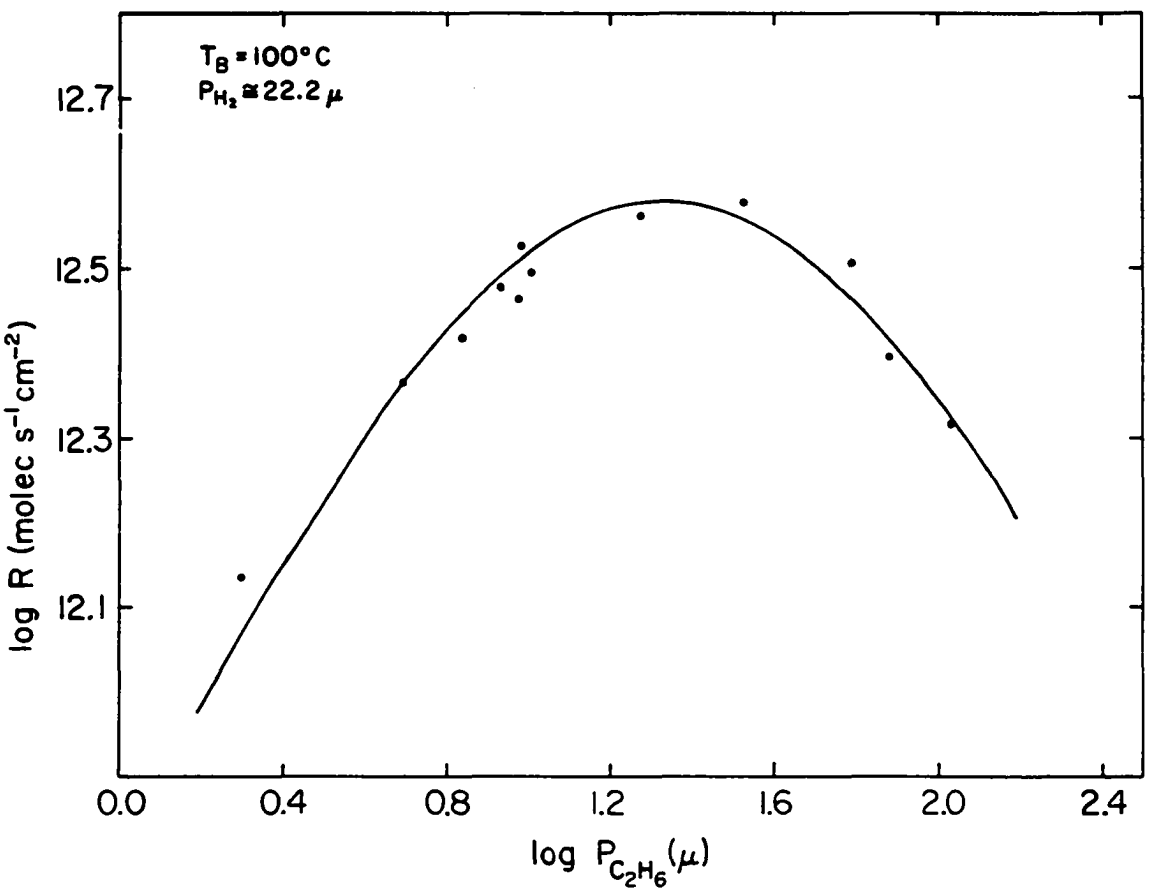

Figure 14. The fit of the hydrogenolysis rate data to (1) is shown at a constant hydrogen pressure which in this case is somewhat higher than in Figure 12. The values of the constants in this fit are a = 1.41 x 10^{-7} $\mu^{1/2}$ cm $s^{1/2}$ $molec^{-1/2}$, b = 2.62 x 10^{-7} cm $s^{1/2}$ $molec^{-1/2}$, c = 0.0 $\mu^{1/2}$ cm $s^{1/2}$ $molec^{-1/2}$ and d = 2.23 x 10^{-7} cm $s^{1/2}$ $molec^{-1/2}$. This film was also deposited at 100°C and the data are corrected for sintering. The actual number of molec. s^{-1} was experimentally determined, then divided by 94.3. 94.3 is the surface area of this catalyst (in cm^2) calculated from a determination of the total number of sites (by a method to be described later) and an assumed area of 10 A^{o2} for each site.

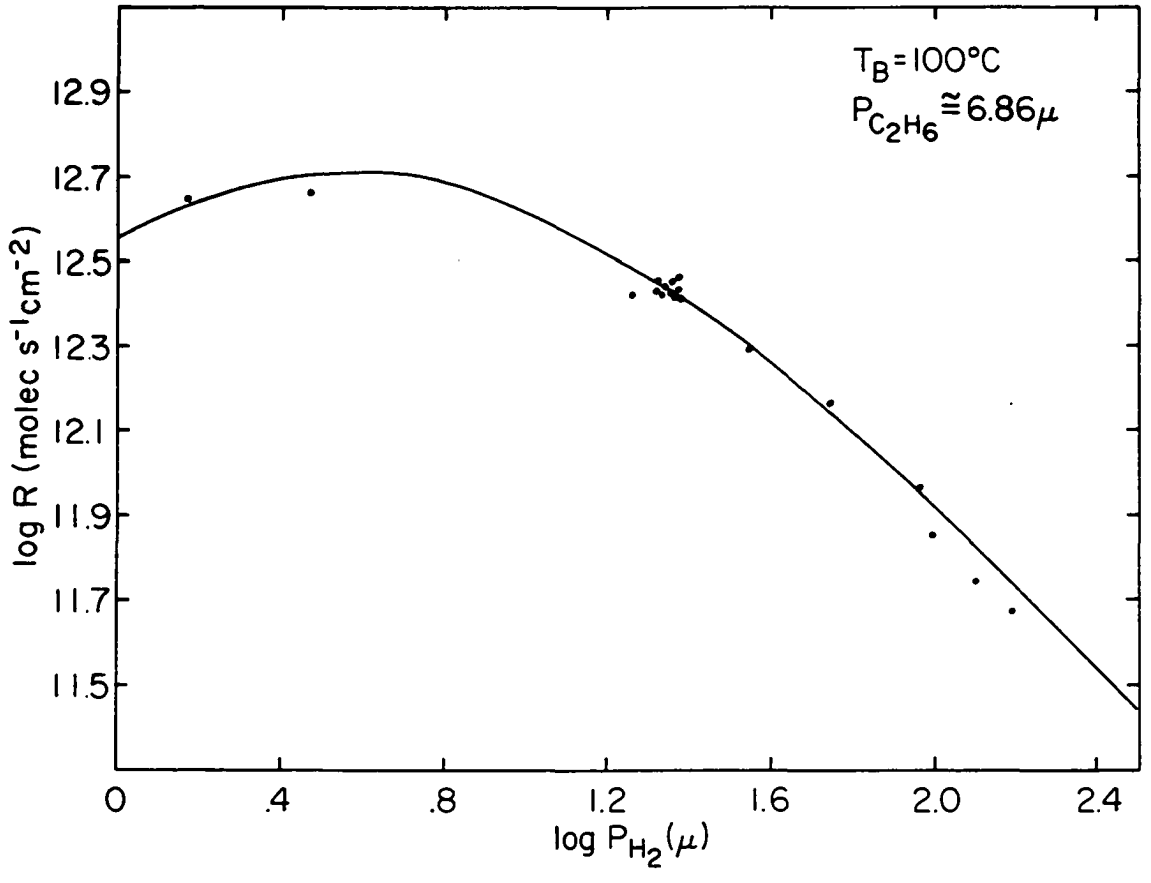

Figure 15. This series of runs is carried out over the film of Figure 14 but at constant ethane pressure. The fit to (1) is shown and the constants are not exactly the same as in Figure 14. Here $a = 1.41 \times 10^{-7}\ \mu^{1/2}$ cm $s^{1/2}$ $molec^{-1/2}$, $b = 1.41 \times 10^{-7}$ cm $s^{1/2}$ $molec^{-1/2}$, $c = 0.0\ \mu^{1/2}$ cm $s^{1/2}$ $molec^{-1/2}$ and $d = 2.66 \times 10^{-7}$ cm $s^{1/2}$ $molec^{-1/2}$. The differences in the values of the constants are attributed to small changes in the thermodynamic properties of the active sites with time as sintering occurs

Although at a bath temperature of 100°C, the constant c is found to be approximately equal to zero in the best fit to the experimental data; this term is left in the rate law (1) because of experiments carried out at 205°C and 170°C. At these temperatures the hydrogenolysis data are fit to a rate law of the same form as equation (1), and here the value of c is not zero. The best fit to the experimental data, in this case, shows the value of b to be close to zero.

The results of these experiments and the fit to equation (1) are shown in Figures 16 and 17 for a bath temperature of 170°C and in Figures 18 and 19 for a bath temperature of 205°C.

Additional results and mechanistic considerations

The kinetic behavior shown above indicates that the ethane hydrogenolysis mechanism involves competition of adsorbed hydrogen and hydrocarbon species for the same surface sites. A hydrogenolysis mechanism which is consistent with several other types of experiments described later and from which can be derived the rate law (1) consists of the following elementary steps.

1. $C_2H_6 + 2\,* \underset{k_{-1}}{\overset{k_1}{\rightleftharpoons}} \begin{matrix} H \\ | \\ H\text{-}C\text{-}H \\ | \\ H\text{-}C\text{-}H \\ | \\ * \end{matrix} + H\,*$

2. $H_2 + 2\,* \underset{k_{-2}}{\overset{k_2}{\rightleftharpoons}} 2\,H\,*$

3. $\begin{matrix} H \\ | \\ H\text{-}C\text{-}H \\ | \\ H\text{-}C\text{-}H \\ | \\ * \end{matrix} + * \underset{k_{-3}}{\overset{k_3}{\rightleftharpoons}} \begin{matrix} H \\ | \\ H\text{-}C\text{-}H \\ | \\ H\text{-}C \\ | \\ * \end{matrix} + H\,*$

Figure 16. The hydrogenolysis rate data and the fit to (1) are shown. In this case no corrections to the experimental rates were necessary because the film was deposited at 225°C and most of the sintering took place during deposition. The values of the constants in (1) were found to be $a = 5.85 \times 10^{-7}\ \mu^{1/2}$ cm $s^{1/2}$ $molec^{-1/2}$, $b = 0.0$ cm $s^{1/2}$ $molec^{-1/2}$, $c = 1.39 \times 10^{-7}\ \mu^{1/2}$ cm $s^{1/2}$ $molec^{-1/2}$ and $d = 6.31 \times 10^{-8}$ cm $s^{1/2}$ $molec^{-1/2}$

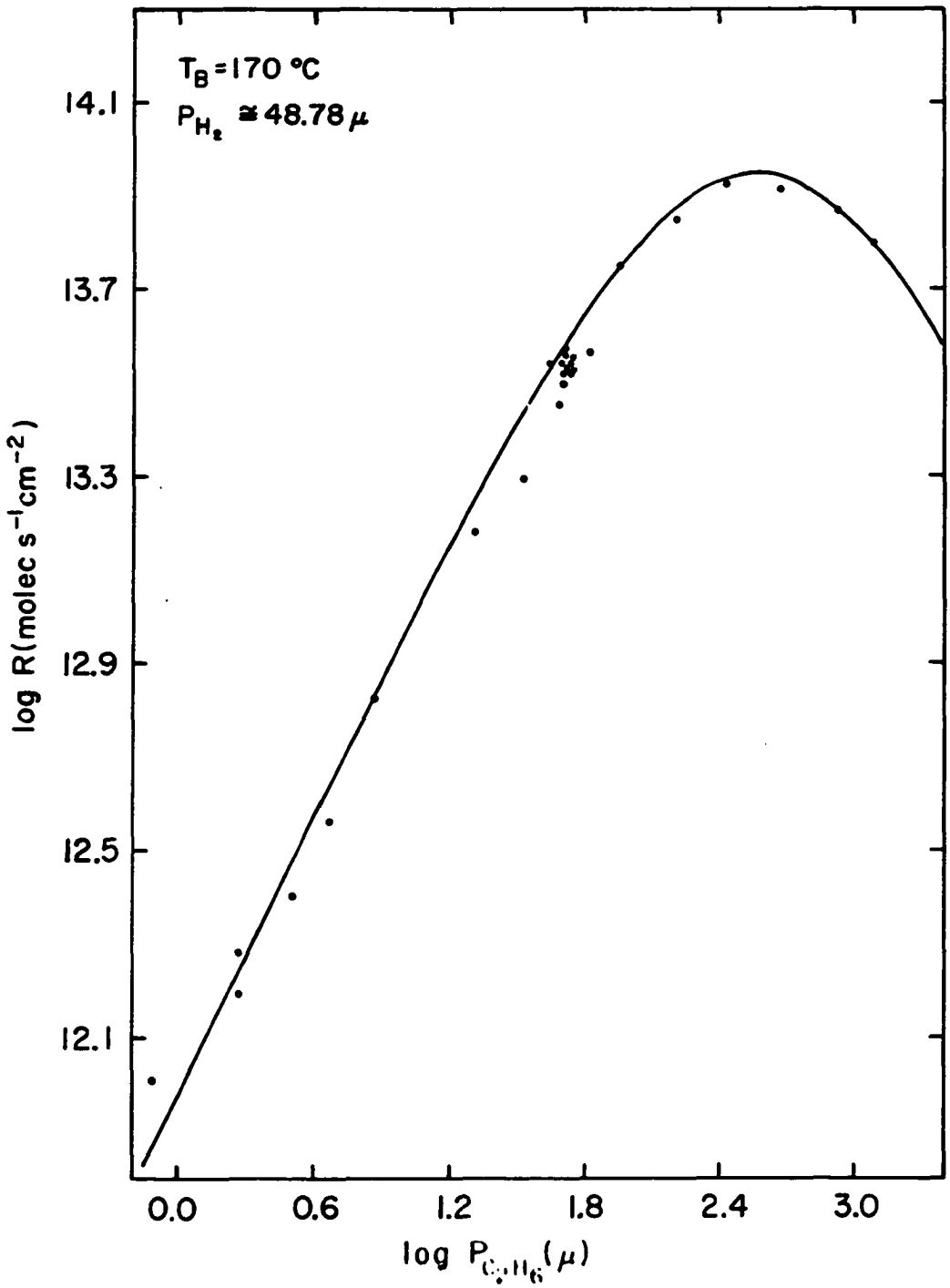
T_B = 170 °C
P_{H_2} ≅ 48.78 μ
14.1
13.7
13.3
12.9
12.5
12.1
log R(molec $s^{-1}cm^{-2}$)
0.0
0.6
1.2
1.8
2.4
3.0
log $P_{C_3H_6}$(μ)

Figure 17. This series of runs was carried out over the film of Figure 16 at 170° and constant ethane pressure. The values of a, b, c and d in the fit to (1) are the same for these two figures

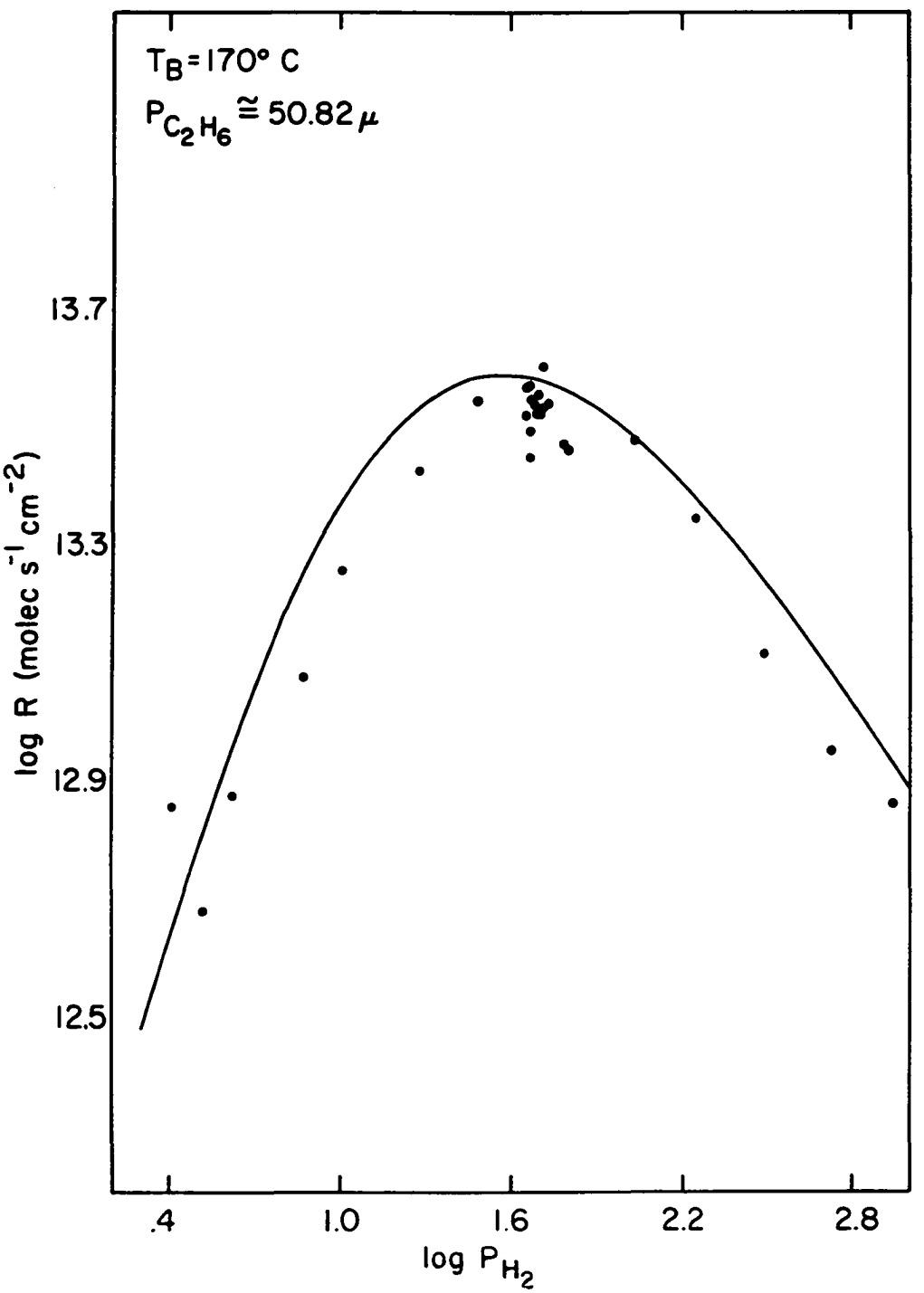
$T_B = 170°$ C
$P_{C_2H_6} \cong 50.82\,\mu$
13.7
13.3
12.9
12.5
log R (molec s^{-1} cm^{-2})
.4
1.0
1.6
2.2
2.8
log P_{H_2}

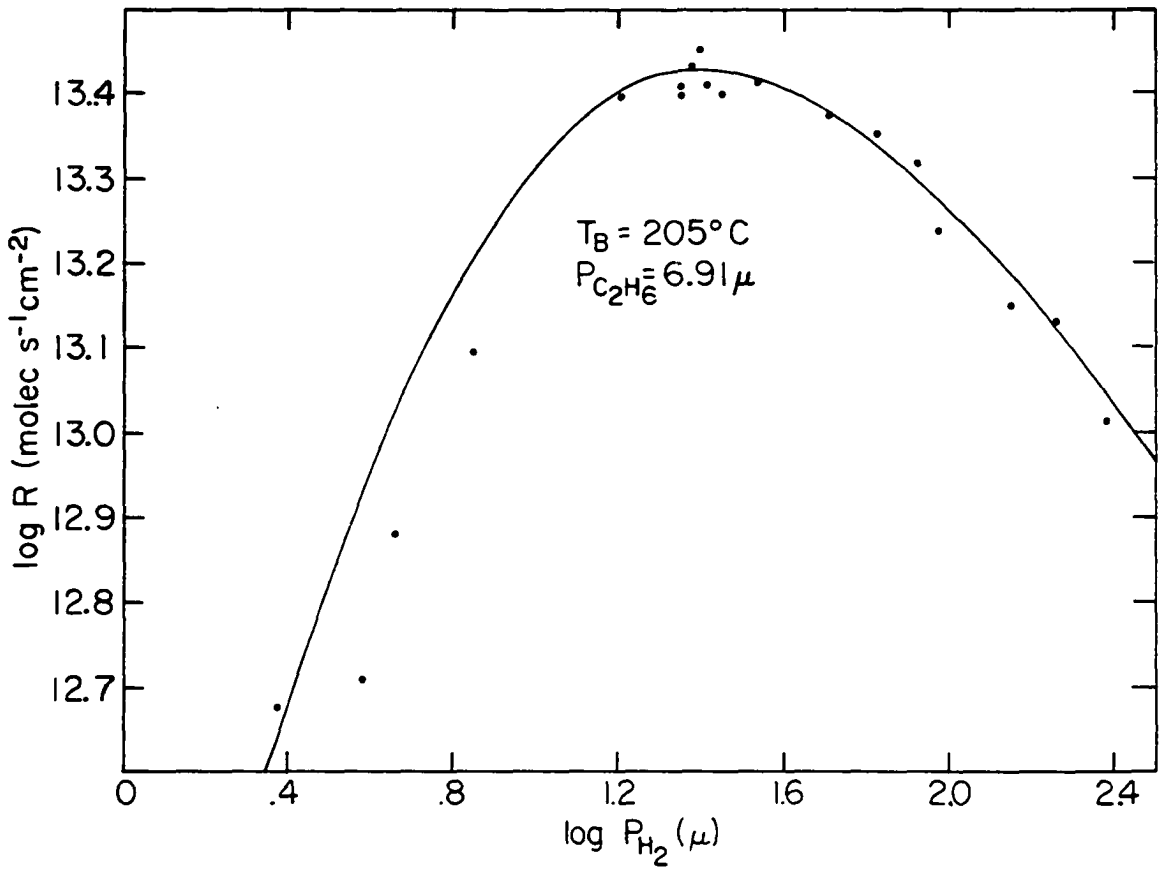

Figure 18. The film, in this case, was deposited at a bath temperature of 205°C and the hydrogenolysis was carried out at this temperature. Runs carried out at standard conditions indicated that only a small correction for sintering was necessary--this was done and the constants of the fit to (1) for the two series of runs represented by Figures 18 and 19 are a = 2.45 x 10^{-7} $\mu^{1/2}$ cm $s^{1/2}$ $moles^{-1/2}$, b = 0.0 cm $s^{1/2}$ $molec^{-1/2}$, c = 3.25 x 10^{-7} $\mu^{1/2}$ cm $s^{1/2}$ $molec^{-1/2}$ and d = 3.45 x 10^{-8} cm $s^{1/2}$ $molec^{-1/2}$. Here the catalytic surface area was 95.5 cm^2 as determined from experiments described later

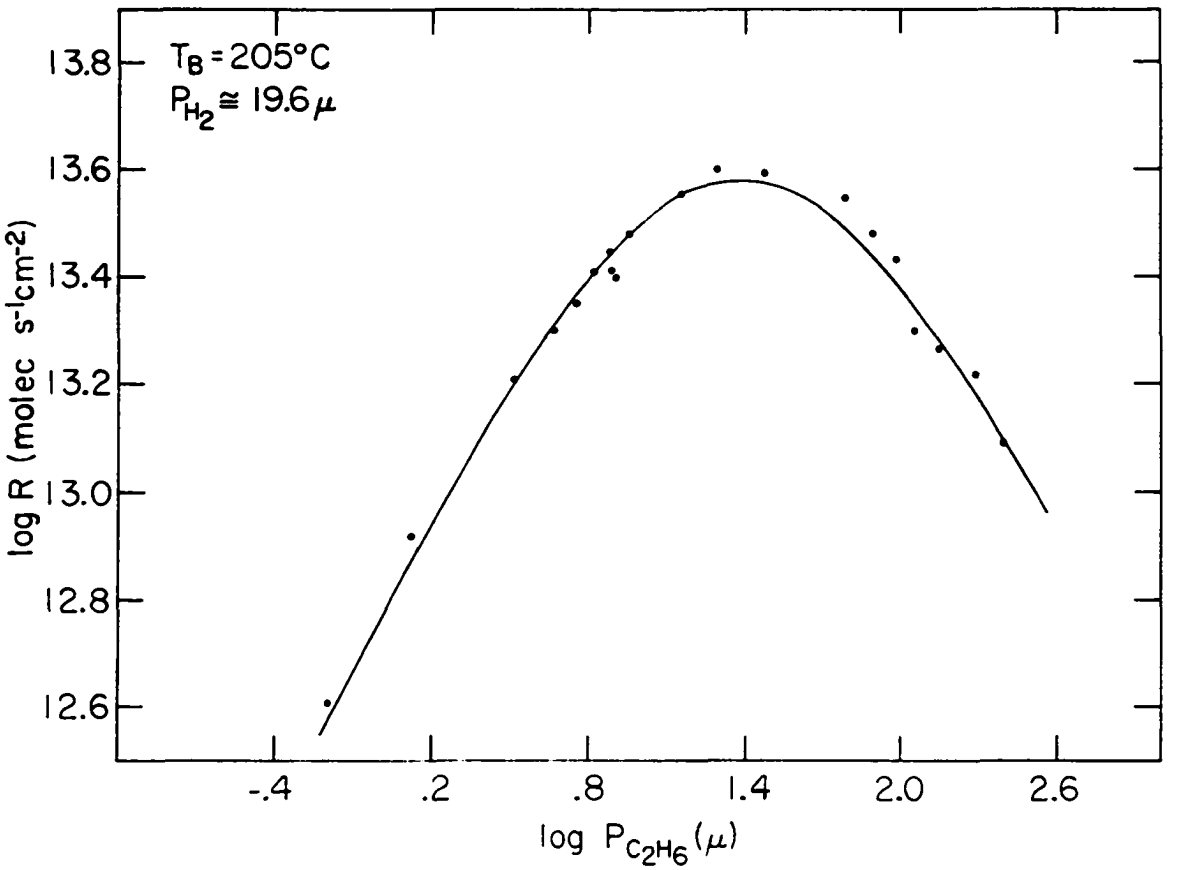

Figure 19. The results of the constant hydrogen pressure series of runs are shown here for the film described in the preceding figure caption and the theoretical curve is based on the same parameter choices

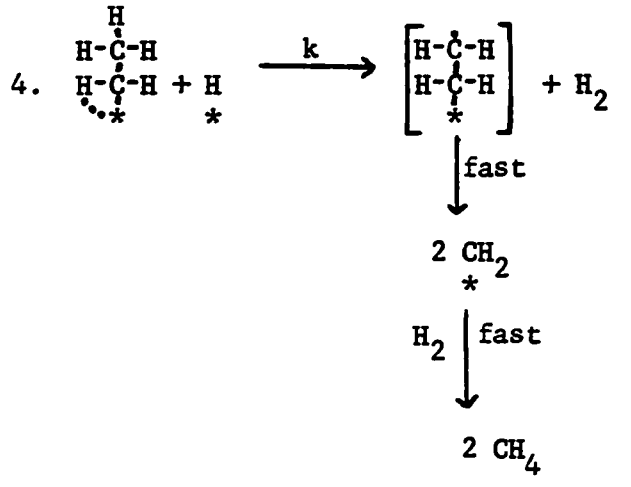

(m)

Ethane is assumed to adsorb in such a way that the remaining two hydrogen atoms, on the carbon atom bonded to the surface, are not equivalent with respect to reaction three. One of these hydrogen atoms (designated by the dotted line to the surface) remains bonded to carbon throughout even though step 3 may take place several times in the forward and reverse directions before either step 4 or the reverse of step 1 takes place.

Although the rate law (1) can be derived in terms of a simple Langmuir type approach, which assumes that step 4 is slow and the surface species H(a), C_2H_4(a) and C_2H_5(a) are all in equilibrium with the gas phase, isotope labeling results described later indicate the need for a more general kinetic treatment which allows for the possibility of nearly irreversible ethane adsorption. Under steady state hydrogenolysis conditions

$$\frac{d\left(\underset{*}{H}\right)}{dt} = \frac{d\left(\underset{*}{C_2H_5}\right)}{dt} = \frac{d\left(\underset{*}{C_2H_4}\right)}{dt} = 0$$

and the total number of sites per unit area of surface, No, is given by

$$No = \left(\underset{*}{C_2H_4}\right) + \left(\underset{*}{C_2H_5}\right) + \left(\underset{*}{H}\right) + (*)$$

From the steady state conditions,

$$1.\quad \frac{d\left(\frac{H}{*}\right)}{dt} = 0 = k_1 (C_2H_6) (*)^2 - k_{-1}\left(\frac{C_2H_5}{*}\right)\left(\frac{H}{*}\right) + k_2 (H_2) (*)^2 - k_{-2}\left(\frac{H}{*}\right)^2 + k_3\left(\frac{C_2H_5}{*}\right)(*) - k_{-3}\left(\frac{C_2H_4}{*}\right)\left(\frac{H}{*}\right) - k\left(\frac{C_2H_5}{*}\right)\left(\frac{H}{*}\right)$$

$$2.\quad \frac{d\left(\frac{C_2H_5}{*}\right)}{dt} = 0 = k_1 (C_2H_6) (*)^2 - k_{-1}\left(\frac{C_2H_5}{*}\right)\left(\frac{H}{*}\right) - k_3\left(\frac{C_2H_5}{*}\right)(*) + k_{-3}\left(\frac{C_2H_4}{*}\right)\left(\frac{H}{*}\right) - k\left(\frac{C_2H_5}{*}\right)\left(\frac{H}{*}\right)$$

$$3.\quad \frac{d\left(\frac{C_2H_4}{*}\right)}{dt} = 0 = k_3\left(\frac{C_2H_5}{*}\right)(*) - k_{-3}\left(\frac{C_2H_4}{*}\right)\left(\frac{H}{*}\right)$$

or

$$\left(\frac{C_2H_4}{*}\right) = \left(\frac{C_2H_5}{*}\right)\left(\frac{k_3/k_{-3}}{\left(\frac{k_2}{k_{-2}}\right)^{1/2}}\right)(H_2)^{1/2} \qquad (n)$$

Addition of equations 2 and 3 gives

$$0 = k_1 (C_2H_6) (*)^2 - k_{-1}\left(\frac{C_2H_5}{*}\right)\left(\frac{H}{*}\right) - k\left(\frac{C_2H_5}{*}\right)\left(\frac{H}{*}\right) \qquad (n')$$

the first equation minus the second minus two times the third gives

$$k_2 (H_2) (*)^2 - k_{-2}\left(\frac{H}{*}\right)^2 = 0$$

or

$$(*) = \left(\frac{H}{*}\right) \Big/ \left(\frac{k_2}{k_{-2}}\right)^{1/2} (H_2)^{1/2} \qquad (n'')$$

Substitution of (n) and (n'') in the equation describing the conservation of sites gives,

$$\left(\frac{H}{*}\right) = \left[\frac{N_o - \left(\frac{C_2H_5}{*}\right)\left(\frac{\left(k_{3/k_{-3}}\right)}{\left(k_{2/k_{-2}}\right)^{1/2}(H_2)^{1/2}} + 1\right)}{\left(1 + \frac{1}{\left(k_{2/k_{-2}}\right)^{1/2}(H_2)^{1/2}}\right)}\right] \qquad (o)$$

Substitution of (n'') then (o) in (n') gives

$$\left(\frac{C_2H_5}{*}\right) = \frac{\left[\frac{k_1 (C_2H_6) N_o}{\left(k_{2/k_{-2}}\right)(H_2)\left(1 + \frac{1}{\left(k_{2/k_{-2}}\right)^{1/2}(H_2)^{1/2}}\right)}\right]}{\left[\frac{k_1 (C_2H_6)\left(\frac{\left(k_{3/k_{-3}}\right)}{\left(k_{2/k_{-2}}\right)^{1/2}(H_2)^{1/2}} + 1\right)}{\left(k_{2/k_{-2}}\right)(H_2)\left(1 + \frac{1}{\left(k_{2/k_{-2}}\right)^{1/2}(H_2)^{1/2}}\right)} + k_{-1} + k\right]} \qquad (p)$$

From step 4 of the reaction mechanism

$$R = k\left(\frac{C_2H_5}{*}\right)\left(\frac{H}{*}\right) = k\left(\frac{C_2H_5}{*}\right)\left[\frac{N_o - \left(\frac{C_2H_5}{*}\right)\left(1 + K_3 / K_2 (H_2)^{1/2}\right)}{\left(1 + 1 / K_2 (H_2)^{1/2}\right)}\right]$$

with

$$K_2 = \left(k_{2/k_{-2}}\right)^{1/2} \qquad K_3 = k_{3/k_{-3}}$$

so that

$$R = \frac{(C_2H_6)}{\left\{ \frac{(k_{-1} + k)^{1/2}}{k_1^{1/2} k^{1/2} N_o} + \frac{k_1^{1/2}}{K_2 k^{1/2} N_o (k_{-1} + k)^{1/2}} \frac{(C_2H_6)}{(H_2)^{1/2}} + \right.}$$

$$\left. \frac{k_1^{1/2} K_3}{K_2^3 k^{1/2} N_o (k_{-1} + k)^{1/2}} \frac{(C_2H_6)}{(H_2)} + \frac{(k_{-1} + k)^{1/2} K_2}{k_1^{1/2} k^{1/2} N_o} (H_2)^{1/2} \right\}^2 \quad (q)$$

giving equation (1)

$$R = \frac{(C_2H_6)}{\left(a + b \frac{(C_2H_6)}{(H_2)^{1/2}} + c \frac{(C_2H_6)}{(H_2)} + d (H_2)^{1/2} \right)^2}$$

with $a = \frac{(k_{-1} + k)^{1/2}}{k_1^{1/2} k^{1/2} N_o}$ $\qquad b = \frac{k_1^{1/2}}{K_2 k^{1/2} N_o (k_{-1} + k)^{1/2}}$

$$c = \frac{k_1^{1/2} K_3}{K_2^3 k^{1/2} N_o (k_{-1} + k)^{1/2}} \qquad d = \frac{(k_{-1} + k)^{1/2} K_2}{k^{1/2} k_1^{1/2} N_o} \quad (q')$$

When the second term in the denominator of (1) is negligible compared to the sum of the other three terms, as is found to be the case at film temperatures of 170°C and 200°C, the concentration of $C_2H_5(a)$ species is much less than the total concentration of sites. On the other hand, at 100°C the third term in the denominator is found to be negligible, corresponding to a very low concentration of $C_2H_4(a)$ species.

It is impossible to determine all of the elementary rate constants from the experimental values of a, b, c and d which are ratios of these constants, since (q′) contains more unknowns than equations. d/a, however, is found to be equal to $K_2 \equiv \left(k_2/k_{-2}\right)^{1/2}$. As expected, K_2 decreases upon

raising the temperature from 100°C (the small increase in the value of K_2 observed on increasing the bath temperature from 170°C to 205°C may be due to the different film pretreatments described in the captions of Figures 16 and 18).

Addition of several microns of methane to a mixture of ethane and hydrogen over a film at 100°C or 205°C does not appreciably change the hydrogenolysis rate. This observation is consistent with the assumption implied by the latter parts of step 4 of (m), that the concentration of single carbon surface species is negligible relative to the concentrations of $C_2H_4(a)$ and $C_2H_5(a)$. The brackets around $\begin{matrix} H\text{-}\dot{C}\text{-}H \\ H\text{-}\dot{C}\text{-}H \\ \cdot\cdot\ \ * \end{matrix}$ are meant to suggest that this species is a very short lived intermediate--all steps following the hydrogen abstraction of reaction 4 are kinetically insignificant if this step is indeed effectively irreversible. $\overset{*}{CH_2}$ is a likely product of the dissociation of this radical, however, production of methane from $\overset{*}{CH_2}$ is not necessarily a single step as the notation might seem to indicate. If it were a single step, CH_2D_2 would be the expected initial product upon addition of D_2 and C_2H_6 to the film. As a matter of fact, a considerable fraction of the initial methane product is CD_4, the exact distribution of deuteromethanes is, however, very difficult to determine because of analytical problems caused by the production of background H_2O, HDO and D_2O in the mass spectrometer.

An example of the isotope labeling results, alluded to as the reason for developing this steady state nonequilibrium treatment, is given below in Table 1. With regard to the adjectives negligible and rapid used in this table, the time scale of the experiments (several hundred seconds) and the sensitivity limitations of the experimental setup described earlier

Table 1. Isotope effects

DOSE D_2 AND C_2H_6

At 25°C (at t ~ 0, $(D_2) \sim 10\ \mu$, $(C_2H_6) \sim 4\ \mu$)

Negligible hydrogenolysis or ethane exchange.

At 100°C (at t ~ 0, $(D_2) \sim 3.6\ \mu$, $(C_2H_6) \sim 3.6\ \mu$)
(look at initial rates)

When the hydrogenolysis rate = $0.00128\ \mu\ s^{-1}$

$$\frac{dP_{C_2H_4D_2}}{dt} = 0.000459\ \mu\ s^{-1}$$

$$\frac{dP_{C_2H_5D}}{dt} = 0.000207\ \mu\ s^{-1}$$

$$0.000666\ \mu\ s^{-1} = \text{exchange rate}$$

Initially a negligible amount of the other isotopes of ethane are produced.

At 205°C or 170°C ($(D_2) \sim (C_2H_6) \sim 15\ \mu$)

Hydrogenolysis is rapid compared to ethane exchange.

---

must be kept in mind. At 100°C the ratio of the rates of hydrogenolysis to exchange is approximately 2 to 1--at 205°C or 170°C this ratio is considerably higher.

With reference to the results at 100°C, the procedure used to separate superimposed cracking patterns of the initial dueteroethanes has been described earlier in the discussion of the experimental procedures, and

subject to the limitations of this method, it was found, in all cases, that the two deuterium atoms of $C_2H_4D_2$ were bound to the same carbon atom. This is the expected result if all the adsorbed hydrocarbon intermediates in the hydrogenolysis are bound to the surface through one carbon atom, as in the reaction scheme (m). Since initially no CH_3-CD_3 species are produced, $C_2H_5(a)$ and $C_2H_4(a)$ are assumed to bond in the manner described in (m).

The ratio of rates of production of $C_2H_4D_2$ to C_2H_5D observed at 100°C in Table 1 is 2.22 and reflects to some degree the ratio of D_2 to H-D over the time period of the exchange rate measurement. If the equilibrium represented by step 3 of reaction scheme (m) was established so fast, that for every $C_2H_5(a)$ species formed from ethane, reaction 3 took place in the forward and reverse directions many times before the adsorbed ethyl species had a chance to desorb as C_2H_6, C_2H_5D or $C_2H_4D_2$, then the ratio of the initial $C_2H_4D_2$ to C_2H_5D production rates would be the same as the ratio of D_2 to H-D, since hydrogen equilibrates very rapidly over the film. This can be seen (if it is assumed that k_{-1}, k_2 and k_{-2} are approximately the same regardless of whether deuterium or hydrogen are involved in these steps) by substituting the appropriate surface concentrations (as given in the derivation of (m)) for $(D_2(g))$, $(H\text{-}D(g))$, $d\,(C_2H_5D)/dt\big|_{t \sim 0}$ and $d\,(C_2H_4D_2)/dt\big|_{t \sim 0}$ whereupon it is found that

$$\frac{(D_2(g))}{(H\text{-}D(g))} = \frac{\binom{D}{*}^2}{2\binom{H}{*}\binom{D}{*}} = \frac{d\,(C_2H_4D_2(g))/dt}{d\,(C_2H_5D(g))/dt}$$

The fact that the D_2 to H-D ratio (over the time period of the 100°C exchange rate measurements of Table 1) was found to be less than 2.0 may

indicate the importance of isotope effects if all the approximations used in the deuteroethane pressure determinations are valid.

Ethane adsorption results

As described earlier, it was necessary to add hydrogen to the reaction chamber following every measurement of the rate in order to remove carbon from the film surface. A consideration of the reaction scheme (m) in light of the results of Table 1 shows that it is indeed to be expected that rapid evacuation of the reaction chamber would leave the hydrocarbon intermediates on the surface. The time scale of the hydrogen equilibration of step 2 is known to be fast compared to the rate of either exchange or hydrogenolysis, since the ratio (H_2) to (H-D) to (D_2) in the gas phase is always close to the statistically expected ratio. Since this is the case, rapid evacuation of the reaction cell will result in a rapid decrease in the surface concentration of hydrogen atoms and the rate of removal of hydrocarbon species from the surface will rapidly fall to zero, since adsorbed hydrogen is involved in both step 4 and the reverse of step 1.

Moreover, the concentration of hydrocarbon species remaining on the catalyst surface following the evacuation of the cell will depend on the partial pressures of ethane and hydrogen just prior to the evacuation. Since these hydrocarbon species are eventually converted to methane upon hydrogen addition, it is expected that the following relationships will hold between the amount of methane produced upon hydrogen addition and the partial pressures of reactants just prior to evacuation of the cell. For a unit reaction volume and surface area, (CH_4) produced

$$= 2\left(\left(\underset{*}{C_2H_5}\right) + \left(\underset{*}{C_2H_4}\right)\right)$$

where these surface concentrations are given by (n) and (p)

$$(CH_4) = 2\left(1 + K_3/K_2(H_2)^{1/2}\right)\left(C_2H_5^*\right)$$

where $K_3 \equiv k_3/k_{-3}$ and $K_2 \equiv \left(k_2/k_{-2}\right)^{1/2}$

$$(CH_4) = \frac{2\left(1 + K_3/K_2(H_2)^{1/2}\right) k_1 (C_2H_6)N_o}{\left[k_1(C_2H_6)\left(1 + K_3/K_2(H_2)^{1/2}\right) + (k_{-1}+k)K_2(H_2)^{1/2}\left(1 + 1/K_2(H_2)^{1/2}\right)\right]} \qquad (r)$$

Most of the constants in (r) can be expressed in terms of b, c and d which are experimentally known from the fit of the hydrogenolysis kinetic data to the rate law (1). When this is done

$$(CH_4) = 2 N_o (C_2H_6) \Big/ \left[(C_2H_6) + \frac{(H_2)\, d\left(1 + 1/K_2(H_2)^{1/2}\right)}{\left(b + cK_2/(H_2)^{1/2}\right)}\right] \qquad (s)$$

For experiments where the hydrogen pressure prior to evacuation was approximately constant and the ethane pressure varied, (s) has the form of a simple Langmuir adsorption isotherm. There are two variables which need to be treated as adjustable parameters in the fit to the experimental data, N_o and K_2 (since b, c and d are known). The fit to experiment is shown in Figure 20 where the ordinate has been normalized (as explained further in the caption) to the values that would be obtained if the surface area was considered to be 1 cm^2 on which 1 x 10^{15} molecules of $C_2H_5^*$ or $C_2H_4^*$ could adsorb in the saturation limit.

This same factor was used to normalize the rate data of Figures 18 and 19 so that R has dimensions molec s^{-1} cm^{-2}. In a similar way the isotherms at 170°C and 100°C were used to determine the hydrocarbon saturation limit

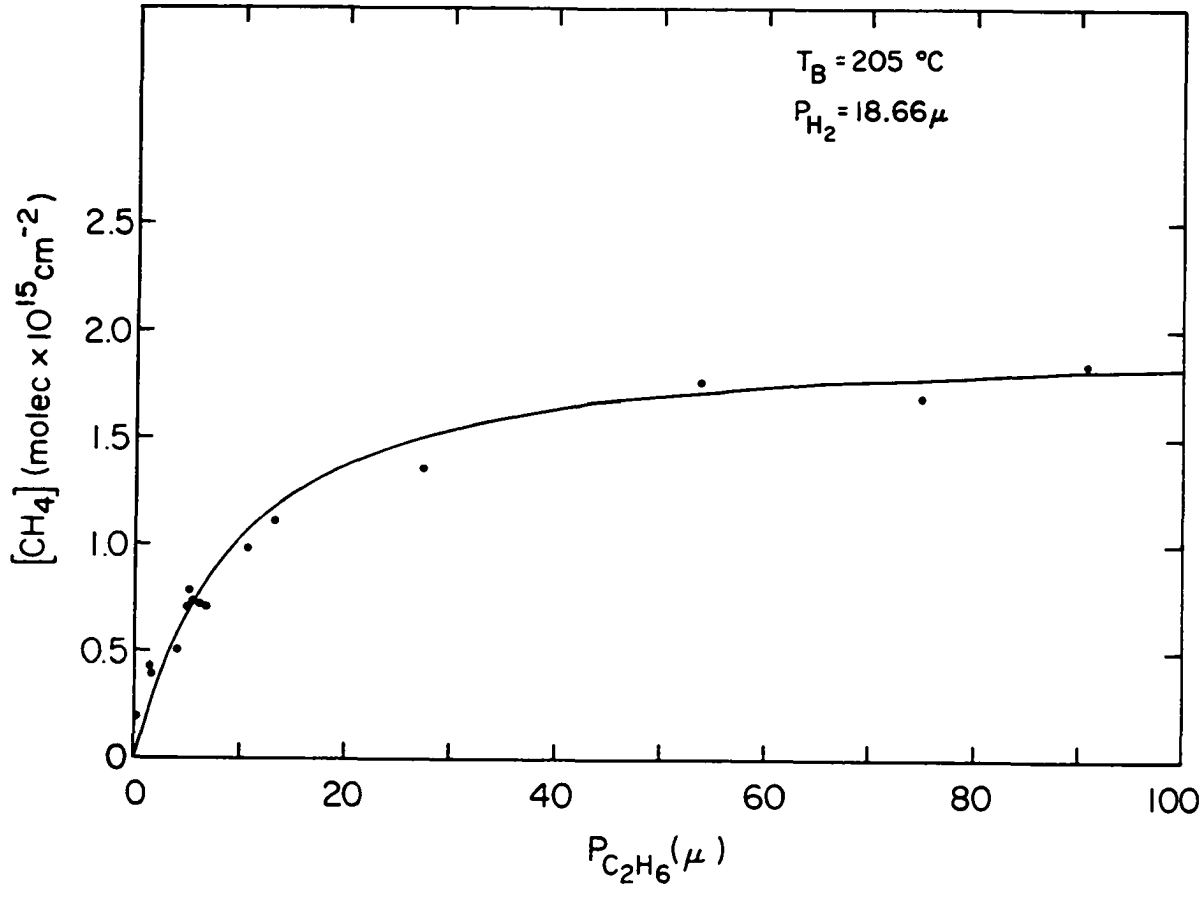

Figure 20. The amount of methane produced upon addition of an excess of hydrogen to the reaction cell is shown as a function of the ethane pressure just prior to the cell evacuation in a preceding hydrogenolysis run. The amount of methane produced allows for a determination of the surface concentrations of C_2H_4 and C_2H_5 during the hydrogenolysis run. The actual amount of methane produced is divided by 95.5 in this figure to produce a saturation limit of 1 x 10^{15} C_2 units on the surface or 2 x 10^{15} methane molecules. This procedure allows for a determination of the surface area, if the area of each site is assumed to be 10 A^{o2}. The fit to (s) is the solid line. The values of b, c and d were obtained from the fit of the hydrogenolysis data to (1) given in the caption of Figure 18, K and N_o are 1.1 and 1 x 10^{15} sites, respectively.

on each of these films, which allows the rates of Figures 14-17 to be expressed in dimensions molec. s^{-1} cm^{-2}.

It is known from the kinetic theory of gases that $3.5 \times 10^{22}\ p/(TM)^{1/2}$ (where P has dimensions mm and M is the molecular weight of the gas) molecules of an ideal gas will strike a square centimeter of surface each second. Since the adsorption isotherms (such as Figure 20) allow for a determination of the number of sites where ethane can adsorb, and since the additional assumption of 10 A^{o2} per site gives the area of these sites, it is possible to determine sticking coefficients of ethane if the total rate of adsorption can be measured. This was done by introducing to the reaction chamber C_2H_6 and simultaneously an amount of D_2 large compared to the number of total sites, then measuring the initial rate of production of hydrogen atoms (as H_2 and H-D) in the gas phase. At 100°C where $C_2H_5^*(a)$ is the most abundant hydrocarbon surface species this rate is set equal to the rate of ethane adsorption, at 205°C (where $C_2H_4(a)$ is rapidly formed) the initial rate of hydrogen atom production is presumed to be twice the rate of ethane chemisorption. The sticking coefficients obtained in this way were found to be very low. For example, at a D_2 pressure of 20 μ and an ethane pressure of 8 μ the sticking coefficient was found to be 1.22×10^{-5} at 100°C and 3.83×10^{-5} at 205°C. These values are consistent with the slow rates of chemisorption of saturated hydrocarbons on transition metals observed by others (63, 64, 65, 66). Our sticking coefficients are not corrected for the fraction of surface covered by adsorbed hydrogen atoms.

Experiments carried out under identical conditions, except for the substitution of H_2 for D_2 and C_2D_6 for C_2H_6, give the sticking coefficient of deuteroethane to be 4.00×10^{-6} at 100°C and 1.38×10^{-5} at 205°C. The

reason for the large isotope effect is not known, but again the results are consistent with similar effects observed for CH_4 and CD_4 adsorption (63, 64).

The counterpart of the data of Figure 20 is shown in Figure 21. Here the dependence of the concentration of surface hydrocarbon species on the partial pressure of hydrogen at constant ethane pressure at 205°C is determined. The constants N_o and K_2 obtained from the best fit to Figure 20 are used in (s) and the resulting fit is shown as the solid line in Figure 21. The poor fit indicates that this treatment is not completely correct.

The following modification of the model was made in order to fit the data of both Figures 20 and 21. It was assumed that on 1 cm^2 of surface (1×10^{15} sites) there were a certain number ($1 \times 10^{15} - N_o'$) of sites on which ethane could adsorb and desorb but not react with hydrogen to split the carbon-carbon bond and form methane. On these sites all rate constants except k were assumed to have the same values as on the N_o' remaining sites. The value of k was assumed to be equal to zero. With these assumptions the form of the right side of (s) is changed by the addition of another term in which N_o is replaced by ($1 \times 10^{15} - N_o'$) and the second term in the denominator is multiplied by $\frac{k_{-1}}{k_{-1} + k}$. The modified isotherm is given below.

$$(CH_4) = \frac{2\,N_o'\,(C_2H_6)}{\left[(C_2H_6) + \dfrac{d(H_2)\left(1 + 1/K_2(H_2)^{1/2}\right)}{\left(b + cK_2/(H_2)^{1/2}\right)}\right]} +$$

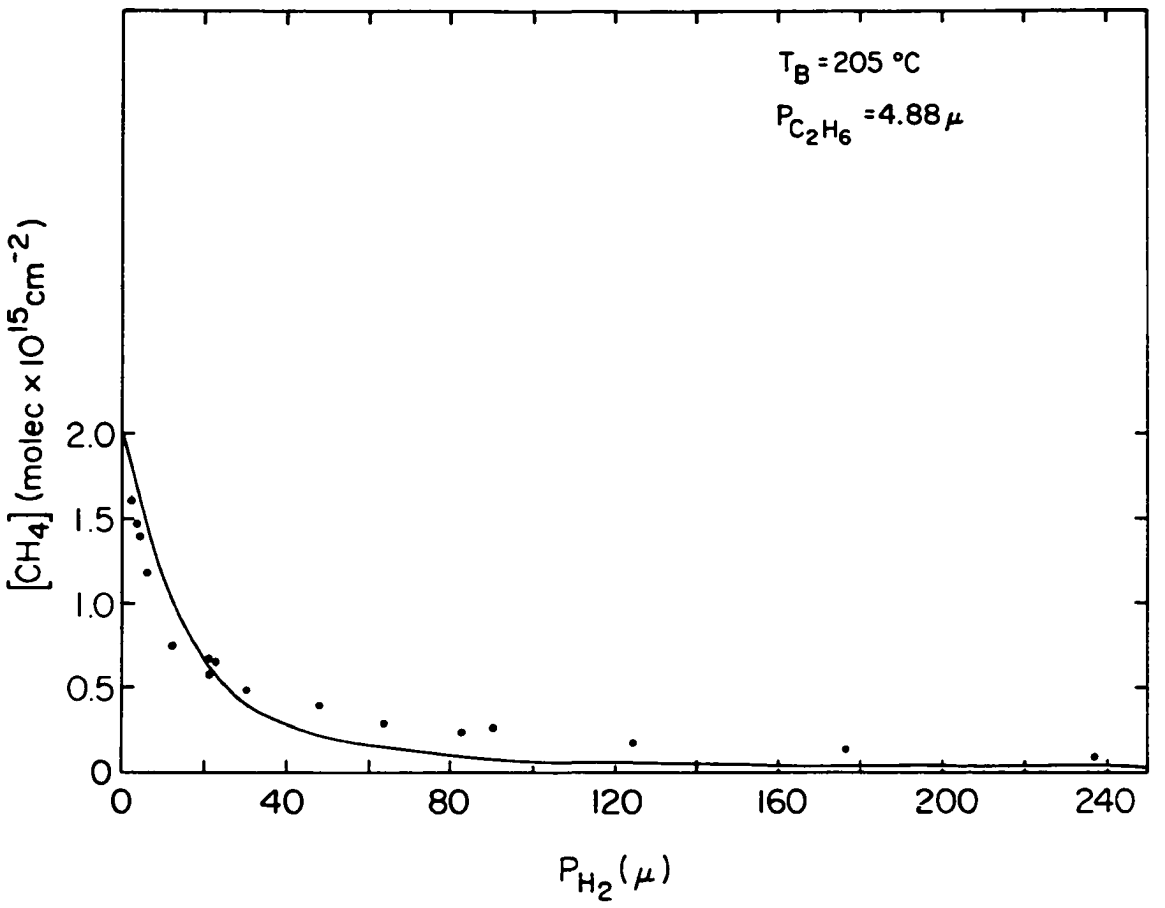

Figure 21. The fit of (s) to the experimental data is shown for the film of Figure 20 but for the case where the ethane pressure was held constant during the hydrogenolysis rate measurements. The poor fit indicates that (s) is the result of an oversimplified treatment

$$\frac{2\,(1 \times 10^{15} - N_o')\,(C_2H_6)}{\left[(C_2H_6) + \frac{k_{-1}\,d}{(k_{-1}+k)}\,\frac{(H_2)\left(1 + 1/K_2(H_2)^{1/2}\right)}{\left(b + cK_2/(H_2)^{1/2}\right)}\right]} \qquad (s')$$

There are now three constants N_o', K_2 and $k_{-1}/(k_{-1}+k)$ which are treated as adjustable parameters in order to get the best fit to two sets of experimental data. The fit to (s′) is found to be satisfactory and is shown in Figures 22 and 23 and in Figures 24 and 25 for a bath temperature of 170°C. Good fits of the experimental isotherms to (s′) were also found at 100°C.

In spite of the apparent agreement between the observed isotherms and (s′), a careful examination of the values of the constants produced in the curve fitting procedure described above indicates that even the treatment leading to (s′) is an oversimplification. For example, from (q′) it is known that $\frac{d}{a} = \left(\frac{k_2}{k_{-2}}\right)^{1/2} \equiv K_2$. However, $\frac{d}{a}$ at a film temperature of 205°C is found to be .141 (from the values of d and a given by the best fit to (1), shown in Figure 19), whereas the value of K_2 (obtained from the fit of (s′) to the isotherms of Figures 22 and 23) is 0.75. Within the framework of the Langmuir type approach which has been used, this discrepancy can be thought of as being due to the assumption that only the value of k differs for the two sets of sites. If the other rate constants are also different for these two sets of sites, the form of the isotherm (s′) would remain the same but the values of the constants in the contribution to (CH_4) from each type of site would not be the same. Since the hydrogenolysis rate data give only constants relating to the active sites, the

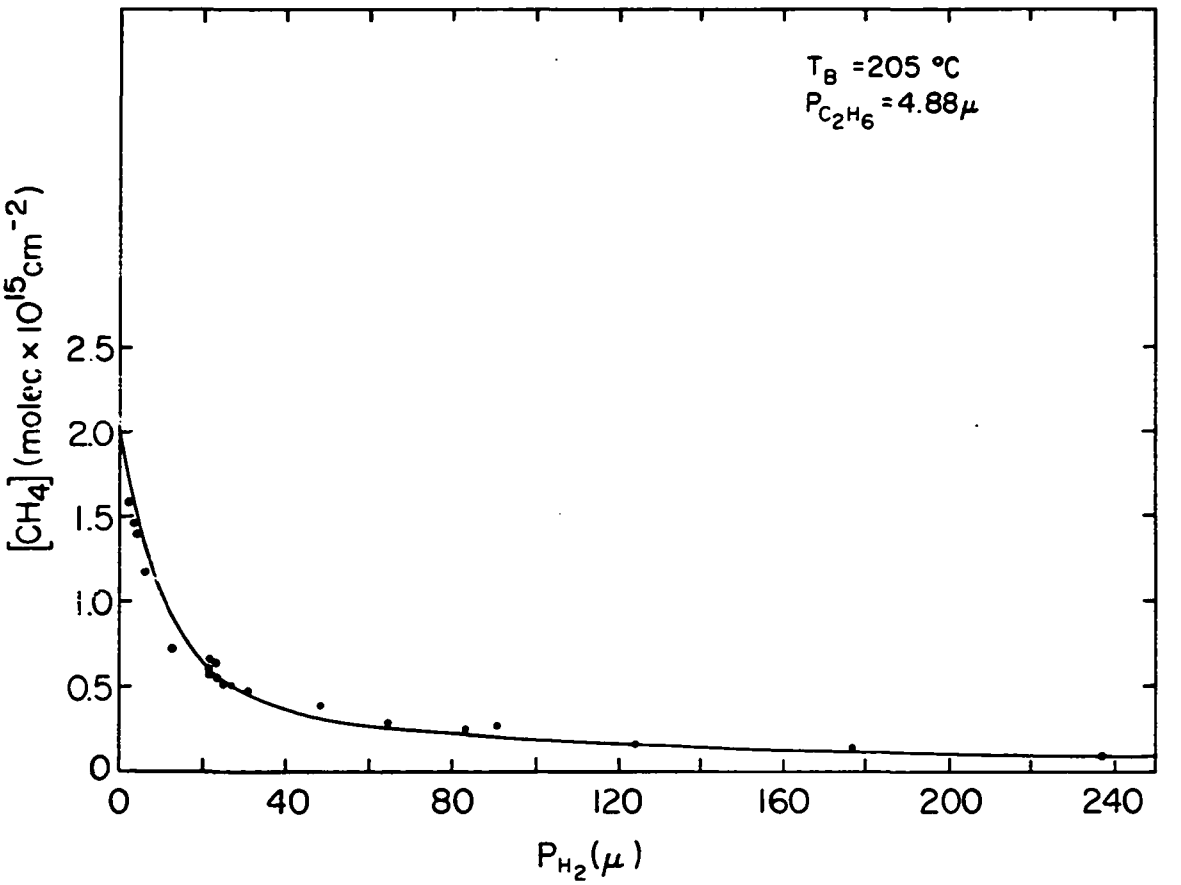

Figure 22. The data of Figure 21 are shown and the fit to (s′). The value values of N_o', K and $\frac{k_{-1}}{k_{-1} + k}$ are 0.85 x 10^{15} sites, .75 and .036, respectively

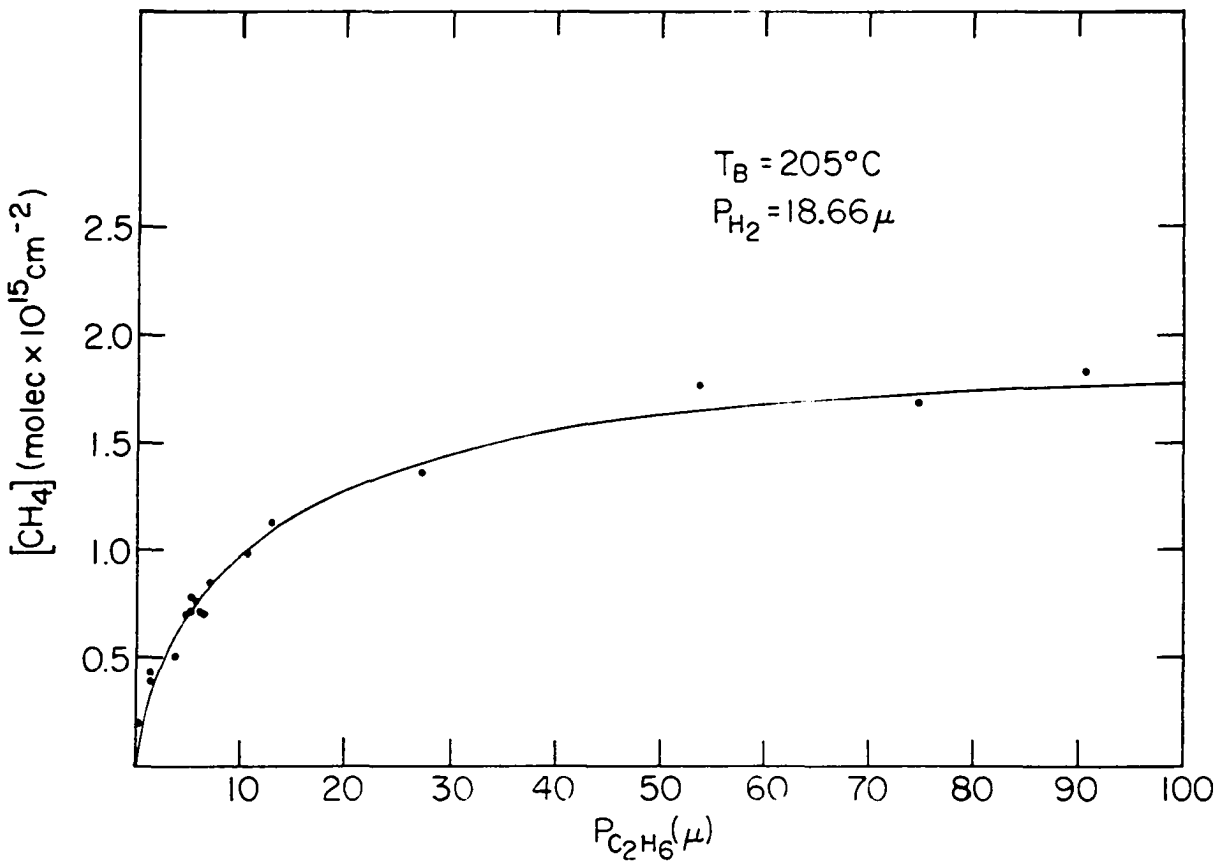

Figure 23. The data of Figure 20 are fit to (s′). The values of the constants which were treated as adjustable parameters to obtain this fit are given in the caption of Figure 22

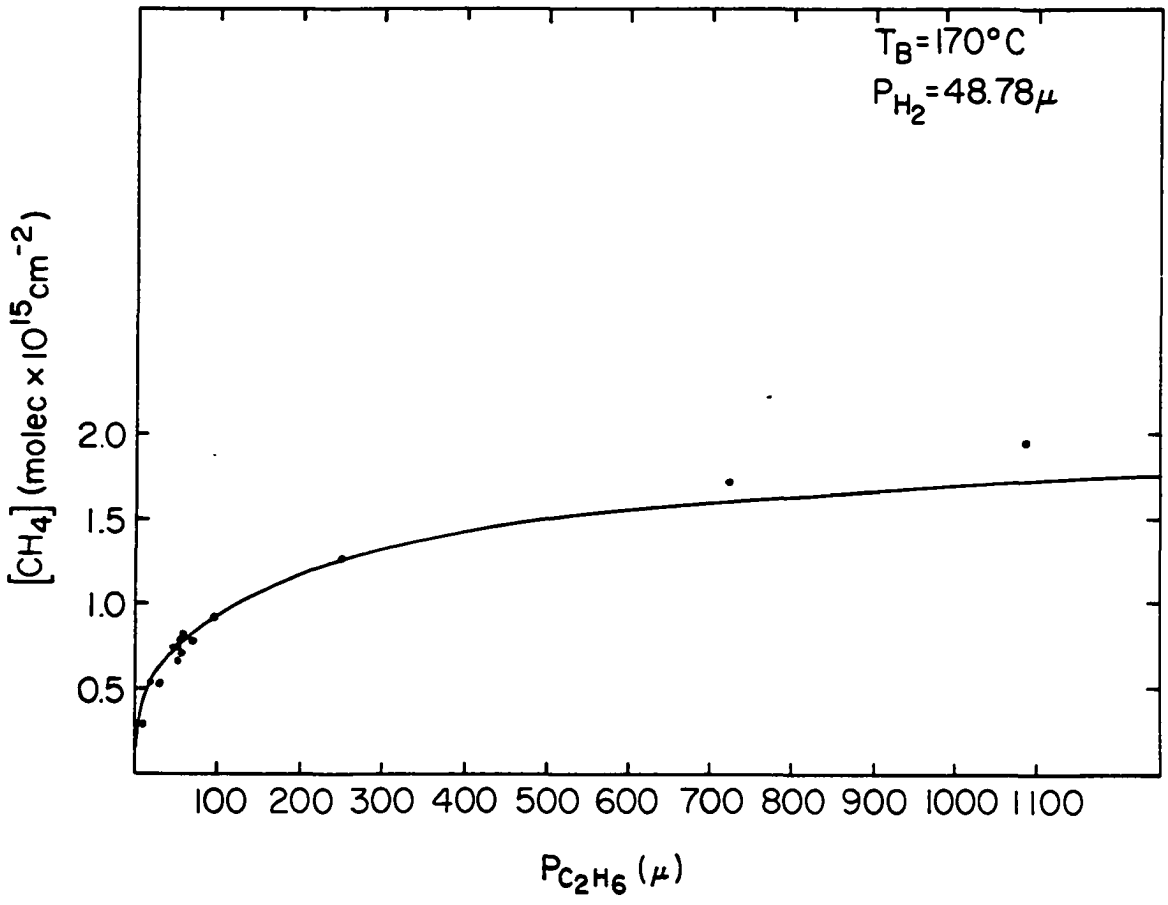

Figure 24. The fit of the isothermal data at 170°C to (s′) is shown where the number of methane molecules experimentally determined has been divided by 37.5 cm^2. The corresponding hydrogenolysis data and the constants b, c and d used in the fit to (s′) are given in Figures 16 and 17. The three remaining adjustable parameters in (s′) were found to be $N_o' = .75 \times 10^{15}$ sites, $K_2 = .75$ and $\frac{k_{-1}}{k_{-1} + k} = .0113$

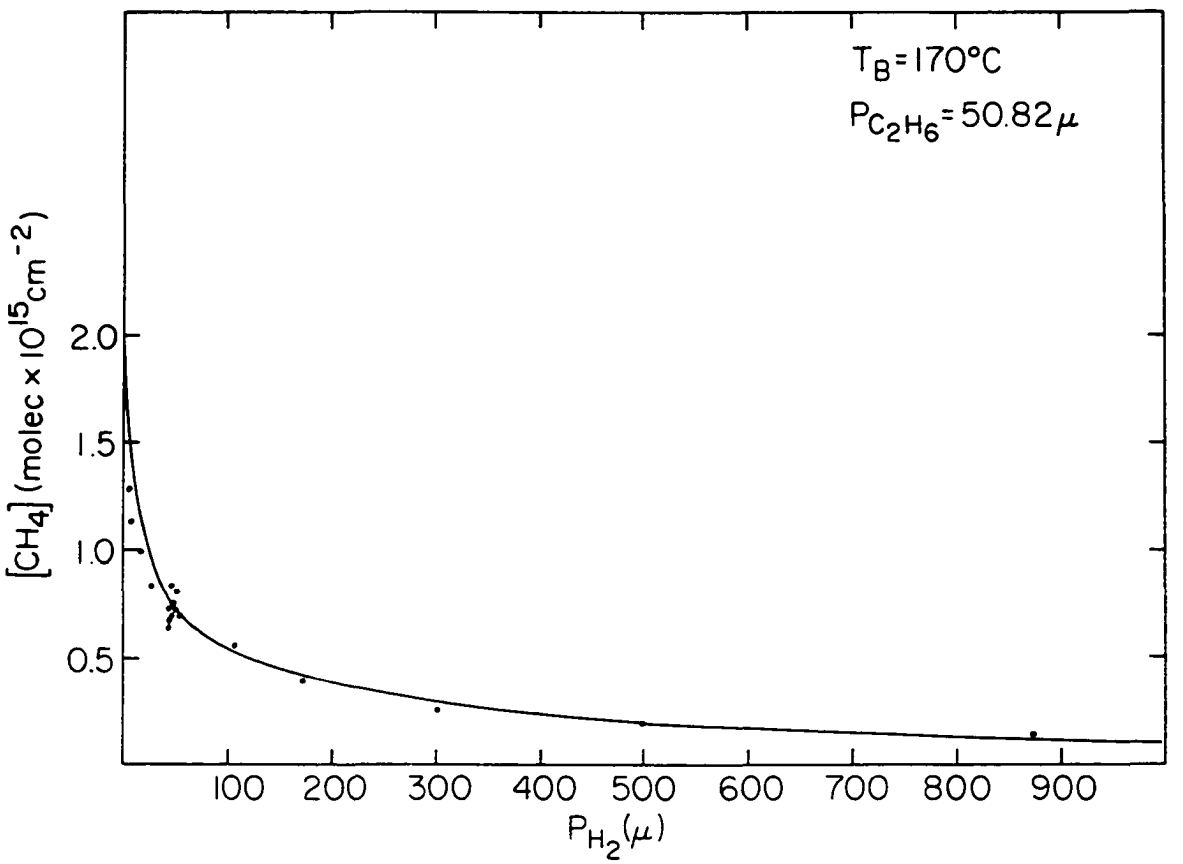

Figure 25. The fit of the 170°C constant ethane pressure data to (s′) is shown. The values of the constants in this equation are given in the caption of the preceding figure

resulting isotherm would have so many adjustable parameters that an accurate determination of their values from the somewhat scattered data would be difficult.

In spite of these qualifications, the fit of (s) and (s′) to the experimental isotherms and the order-of-magnitude agreement between K_2 and d/a (determined from fits to isothermal and hydrogenolysis rate data, respectively) indicate that surface concentrations of hydrogen and hydrocarbon species depend on gas phase pressures in a way that is at least qualitatively expected from a consideration of the proposed hydrogenolysis mechanism and that in addition much of the surface on which ethane adsorbs is catalytically active.

The significance of the estimate of the number of active sites by method (s) (or more accurately by (s′)) is that hydrogenolysis rates can be expressed as turnover numbers (having dimensions molec. s^{-1} $site^{-1}$) and a direct comparison can be made of the activities of different catalysts. In particular, it is instructive to compare the turnover numbers of thin films deposited at different temperatures. For example, if rates measured at 100°C (over a thin film deposited at 100°C) are converted to turnover numbers (using N_o' values obtained from (s′)) and extrapolated to 205°C using the apparent activation energy of Figure 10, it is found that these turnover numbers are more than two orders of magnitude greater than those experimentally observed at 205°C. Similarly, the turnover number measured at 100°C, in the case where the thin film has been extensively sintered during deposition, is considerably lower than the turnover number obtained at the same partial pressure of ethane and hydrogen but over a film deposited at 100°C.

These observations indicate that in addition to the reduction in the number of active sites, a significant irreversible change in the structure of the active sites takes place upon annealing for short periods of time at temperatures at or above 200°C. This change probably involves the transformation of a (at least partially) disordered "amorphous type" structure to a more ordered but less catalytically active "crystalline type" structure. Support for this viewpoint comes from results obtained over the single crystal catalysts. It is well known from L.E.E.D. studies that Ar^+ bombardment will disorder a transition metal surface. The order can, however, rapidly be restored by annealing for several minutes at several hundred degrees centigrade. The catalytic activity of the iridium single crystal surfaces (the (100), (110), (111) and (321) faces) which were well annealed following ion bombardment was found to be so low (for crystal temperatures of 400°C or lower) that upon introduction of $\sim$ 10 μ of ethane and $\sim$ 10 μ of hydrogen to the reaction chamber, no change in partial pressures could be measured over a time period of $\sim$ 1,000 s. On the other hand, if the single crystal discs were not annealed following bombardment, a small degree of catalytic activity could be observed, which quickly diminished at, for example, 200°C as the surface reordered.

It must be concluded from these results that there are significant differences in the properties of the well annealed single crystal (100), (110), (111) and (321) surfaces, the catalytically most active sites of films deposited at 100°C and those sites of films deposited at 200°C-230°C. A detailed investigation of the nature of these differences would require supplemental surface sensitive techniques of the type described below.

SUMMARY AND SUGGESTIONS AS TO THE DIRECTION FOR FUTURE INVESTIGATION

The interactions of hydrogen with ethylene and ethane over iridium catalysts have been studied using a combination of kinetic and isotope labeling experiments. Hydrogenation and hydrogenolysis mechanisms are proposed, which within the framework of a simple Langmuir type approach account for the experimental results in a self-consistent way. The Langmuir type approach, which does not account for surface heterogenity or interactions between adsorbed species, is nevertheless used as a first approximation, in the absence of detailed information concerning the properties of adsorbed species.

Although surface hydrocarbon species of varying composition are proposed in this study, the nature of the experimental approach is such that only a limited amount of information concerning the electronic and geometric structure of these intermediates can be obtained. The surface sensitive techniques of ultraviolet photoelectron spectroscopy, low energy electron diffraction and Auger electron spectroscopy could provide a direct probe of the structure of the catalytic surface and the adsorbed species. The author has found no such work published for ethane adsorbed on any transition metal surface. Of particular interest would be such a study where these surfaces were nonannealed iridium thin films, annealed thin films and single crystal surfaces.

A study of ethane hydrogenolysis over transition metal surfaces other than iridium is needed in order to determine the degree of generality of the kinetic behavior observed in this study.

BIBLIOGRAPHY

1. P. Mahaffy, P. B. Masterson and R. S. Hansen, J. Chem. Phys. 64, 3911 (1976).

2. P. B. Masterson, Ph.D. thesis, Iowa State University, (1971) (unpublished).

3. P. Sabatier and J. B. Senderens, C. R. 124, 1358 (1897).

4. D. D. Eley and J. L. Tuck, Trans. Farad. Soc. 32, 1425 (1936).

5. E. S. Giffillan and M. Ploanyi, Z. Phisik. Chem. A1^{c}6, 254 (1933).

6. S. J. Thomson and J. L. Wishlade, Trans. Farad. Soc. 58, 1170 (1962).

7. D. Cormack, S. J. Thomson and G. Webb, J. Catal. 5, 224 (1966).

8. O. Beeck, Rev. Mod. Phys. 17, 61 (1945).

9. J. Horiuti and K. Miyahara, Natl. Bur. Stand. Ref. Data Ser. 13, 1 (1968).

10. G. C. Bond, Adv. Cat. 15, 91 (1965).

11. O. Toyoma, Rev. Phys. Chem. Japan 9, 123 (1935).

12. G. I. Jenkins and E. K. Rideal, J. Chem. Soc., 2490 (1955).

13. O. Beeck, Disc. Farad. Soc. 8, 118 (1950).

14. B. M. W. Trapnell, Trans. Farad. Soc. 48, 160 (1952).

15. R. W. Roberts, J. Phys. Chem. 68, 2718 (1964).

16. K. Miyahara, J. Res. Inst. Cat., Hokkaido Univ. 14, 134 (1966).

17. J. G. Foss and H. Eyring, J. Phys. Chem. 62, 103 (1958).

18. H. zur Strassen, Z. Phys. Chem. (Leipzig) A169, 81 (1934).

19. J. Horiuti, J. Res. Inst. Cat., Hokkaido Univ. 6, 250 (1958).

20. K. Miyahara, S. Oki, K. Harada and K. Nagai, J. Res. Inst. Cata., Hokkaido Univer. 16, 555 (1968).

21. C. Kemball, J. Chem. Soc., 735 (1956).

22. R. Rye, J. Res. Inst. Cat., Hokkaido Univ. 17, 223 (1969).

23. R. Rye and R. S. Hansen, J. Chem. Phys. 50, 3585 (1969).

24. R. Rye and R. S. Hansen, J. Phys. Chem. 73, 1667 (1969).

25. G. I. Jenkins and E. K. Rideal, J. Chem. Soc., 2496 (1955).

26. E. K. Rideal, Proc. Camb. Phil. Soc. 35, 1301 (1939).

27. E. K. Rideal and G. H. Twigg, Proc. Roy. Soc. 171A, 55 (1939).

28. N. C. Gardner and R. S. Hansen, J. Phys. Chem. 74, 3298 (1970).

29. S. J. Thomson and G. Webb, J. Chem. Soc. Chem. Comm., 526 (1967).

30. G. H. Twigg, Disc. Farad. Soc. 8, 152 (1950).

31. J. Horiuti and M. Polanyi, Trans. Farad. Soc. 30, 1164 (1934).

32. R. P. Eischens and W. A. Pliskin, Adv. Catal. 10, 1 (1958).

33. J. B. Peri, Disc. Farad. Soc. 41, 121 (1966).

34. G. Bleyholder and W. V. Wyatt, J. Phys. Chem. 76, 618 (1974).

35. J. E. Demuth and D. E. Eastman, Phys. Rev. Letters 32, 1123 (1974).

36. N. Rösch and T. Rhodin, Phys. Rev. Letters 32, 1189 (1974).

37. W. H. Weinberg, H. A. Deans and R. P. Merril, Surf. Sci. 14, 312 (1974).

38. K. Baron, D. Blakely and G. A. Somorjai, Surf. Sci. 41, 45 (1974).

39. D. Hagen, B. Nieuwenhuys, G. Rovida and G. A. Somorjai, Surf. Sci. 59, 155 (1976).

40. J. R. Arthur and R. S. Hansen, J. Chem. Phys. 36, 2062 (1962).

41. R. S. Hansen, J. R. Arthur, V. J. Mimeault and R. Rye, J. Phys. Chem. 70, 2787 (1966).

42. P. Franken and V. Ponec, Surf. Sci. 53, 341 (1975).

43. C. Kemball and H. S. Taylor, J. Am. Chem. Soc. 70, 345 (1948).

44. A. Cimino, M. Boudart and H. S. Taylor, J. Phys. Chem. 58, 796 (1954).

45. J. H. Sinfelt, Cat. Rev. 7, 91 (1973).

46. J. H. Sinfelt, Cat. Rev. 3, 175 (1969).

47. J. H. Sinfelt, W. F. Taylor and D. J. C. Yates, J. Phys. Chem. 69, 95 (1965).

48. J. H. Sinfelt and D. J. C. Yates, J. Cat. 8, 82 (1967).

49. J. H. Sinfelt and D. J. C. Yates, J. Cat. 10, 362 (1968).

50. D. J. C. Yates and J. H. Sinfelt, J. Cat. 14, 182 (1969).

51. J. H. Sinfelt and W. F. Taylor, Trans. Farad. Soc. 61, 20 (1965).

52. C. Kemball, Disc. Farad. Soc. 41, 190 (1966).

53. M. Boudart, A. I. Ch. E. Journal 18, 465 (1972).

54. S. Khammouma, Ph.D. thesis, Stanford University, (1972) (unpublished).

55. J. R. Anderson and B. G. Baker, Proc. Roy. Soc. 271A, 402 (1963).

56. L. Guczi, B. S. Gudkov and P. Tetenyi, J. Cat. 24, 187 (1972).

57. Y. Amenomiya and R. F. Pottie, Can. J. Chem. 46, 1741 (1968).

58. E. Quinn and F. Mohler, J. Rs. Natl. Bur. Stand. 65A, 93 (1961).

59. R. J. Kokes, Cat. Rev. 6, 1 (1972).

60. J. H. Sinfelt, J. Cat. 27, 468 (1972).

61. R. W. Roberts, J. Phys. Chem. 67, 2035 (1963).

62. R. S. Dowie, C. Kemball and D. A. Whan, J. Phys. Chem. 80, 2900 (1976).

63. H. F. Winters, J. Chem. Phys. 62, 2454 (1975).

64. C. Stewart and G. Ehrlich, J. Chem. Phys. 62, 4672 (1975).

65. T. Madey, Surf. Sci. 29, 571 (1972).

66. J. T. Yates and T. Madey, Surf. Sci. 28, 437 (1971).

ACKNOWLEDGMENTS

The author would like to thank Dr. R. S. Hansen and the "dry" members of Physical and Inorganic Group III for their interest and assistance in this research project.

Thanks goes out to Mr. Martin Strasburger and Dr. R. Lambert for their assistance in the numerical integration of equation (k) and to Mr. William Frazier who helped construct and "debug" several programs. The help of the members of the glass shop in their skillful construction of many reaction cells is gratefully acknowledged.

I would like to thank my parents for the part they played in my early education and Dr. R. Maatman of Dordt College who initially stimulated my interest in catalysis.

The continued interest of my brother, Pete, in this work is appreciated as is the moral support provided by the rest of my family, including Sam and Kay who supplied a warm place to sleep on many occasions when I passed through Ann Arbor. Finally I would like to thank Judith DeJong for her encouragement, support and patience (particularly in putting up with many poor puns).